2.7. Preparation of cured cells

To prepare cured cells, HCV RNA-replicating cells were treated with IFN-α or IFN-γ as described previously (Abe et al., 2005; Ikeda et al., 2005; Naka et al., 2005). Briefly, the cells (each 1×10^6) were treated with IFN-α or IFN-γ (each 500 IU/ml) in the absence of G418. The treatment was continued for 3 weeks with the addition of IFN at 4-day intervals. The cured cells obtained from sO, O, OA, OB, OD, and OE cells (HCV RNA-replicating cells obtained in this study, see Fig. 2A) were named sOc, Oc, OAc, OBc, ODc, and OEc, respectively, and were cultured in DMEM supplemented with 10% fetal bovine serum in the absence of G418. RT-PCR confirmed the absence of HCV RNA in these cured cells.

2.8. Reverse transcription-polymerase chain reaction (RT-PCR)

To amplify HCV RNA, RT-PCR was carried out separately in two parts as described previously (Ikeda et al., 2005). Briefly, one part covered from HCV 5′-UTR to NS3, with a final product of approximately 5.1 kb, and the other part covered from NS2 to most of HCV 3′-UTR, with a final product of approximately 6.1 kb. These fragments overlapped at the NS2 and NS3 regions and were used for sequence analysis for HCV open reading frame (ORF) after cloning into pBR322MC (Kishine et al., 2002). SuperScript II (Invitrogen) and KOD-plus DNA polymerase (Toyobo, Osaka, Japan) were used for RT and PCR, respectively.

2.9. cDNA cloning and sequencing

Two PCR products (5.1 and 6.1 kb) were digested with *Xba*I and then cloned into the *Xba*I site of pBR322MC, as described previously (Kato et al., 2005). Plasmid insertions were sequenced in both the sense and antisense directions using the Big Dye Terminator Cycle Sequencing kit (Perkin–Elmer Life Sciences) on an ABI PRISM 310 genetic analyzer (Applied Biosystems, Foster City, CA).

2.10. Transient replication assays

The cells were transfected with 20 μg RNA by electroporation as described above. After electroporation, the cells were plated onto 24-well plates at 3×10^4 cells per well. The cells were harvested with Renilla lysis reagent (Promega, Madison, WI) at 24, 48, 72, and 96 h after the electroporation, and were subjected to luciferase assay according to the manufacturer's protocol.

2.11. Molecular evolutionary analysis

Nucleotide sequences (10,972 nucleotides of HCV 5′-UTR to NS5B) of clones obtained by RT-PCRs from O, OA, OB, OD, and OE cells were analyzed by neighbor-joining analysis using the program GENETYX-MAC (Software Development, Tokyo, Japan).

3. Results

3.1. Establishment of genome-length HCV RNA-replicating cell lines

We previously established a cloned sO cell line possessing a subgenomic HCV replicon (O strain) and found an adaptive mutation (S2200R) in NS5A (Kato and Sugiyama et al., 2003). More recently we further established a cloned O cell line replicating genome-length HCV RNA by the selection with G418 treatment following the electroporation of genome-length HCV RNA with the S2200R mutation into sOc cured cells (Ikeda et al., 2005). In that study, we found a second adaptive mutation (K1609E) in the NS3 helicase region of HCV RNA-replicating in the O cells, and we also observed that the Oc cured cells showed more overwhelming advantages than the sOc cells in the replication of genome-length HCV RNA (Ikeda et al., 2005). These results suggested that the K1609E mutation was required for the robust replication of genome-length HCV RNA, and that cell backgrounds regarding the potentials of RNA replication differ greatly between sOc and Oc cells. However, we could not clarify whether or not K1609E is the unique or best adaptive mutation for RNA replication. Furthermore, we obtained no information indicating whether viral or host factors are the main contributors to the robust RNA replication.

To obtain such information, we attempted to establish additional genome-length HCV RNA-replicating cell lines by the electroporation of ON/C-5B RNA, which possesses the S2200R mutation (Fig. 1), into sOc or Oc cells (Fig. 2A). After 3 weeks of G418 selection, we obtained one G418-resistant colony derived from sOc cells and three G418-resistant colonies derived from Oc cells. These G418-resistant colonies proliferated successfully; the sOc-derived colony was named OA cell line and Oc-derived three colonies were called OB, OD, and OE cell lines (Fig. 2A), and then these cell lines were used for further analysis. To examine the replication level of genome-length HCV RNA in these cell lines, total RNAs and proteins extracted from OA, OB, OD, and OE cells were subjected to Northern and Western blot analyses, respectively. Total RNAs and proteins extracted from the O, sOc, and Oc cells were also used for the comparison. Genome-length HCV RNAs approximately 11 kb long were detected in all specimens except those from the sOc and Oc cells (Fig. 2B). The number of copies of HCV RNAs in total RNA (each 3 μg) was estimated to be more than 10^7 by comparing these HCV RNAs with HCV RNA synthesized in vitro, although the levels in OB and OD cells were somewhat lower than those in O, OA, and OE cells. The core was also detected in all specimens except those from the sOc and Oc cells (Fig. 2C). The levels of the core in OB and OD cells were also somewhat lower than those in O, OA, and OE cells. These results suggest that the replication levels of HCV RNA in OA cells are equivalent to that in O cells and are higher than those in OB, OD, and OE cells. Although the expression of HCV RNAs and HCV proteins differed somewhat among these cell lines, these lines, including that of O cells, were maintained for at least several months in the presence of G418 (data not shown), suggesting the stable robust HCV RNA replication. The OA, OB, OD, and OE cells

were highly sensitive to IFN-α towards HCV RNA replication (data not shown), as were the O cells (Ikeda et al., 2005; Naka et al., 2005).

3.2. Genetic analysis of HCV RNAs replicating in the OA, OB, OD, and OE cells and comparison with that in the O cells

To learn whether or not HCV RNAs replicating in the OA, OB, OD, and OE cells possess the K1609E mutation, we performed sequence analysis of HCV RNAs replicating in these cell lines. Total RNAs extracted from these cells were subjected to RT-PCR, and then two fragments (5.1 and 6.1 kb) amplified by RT-PCR for ORF were subcloned into plasmid for sequence analysis, as described previously (Ikeda et al., 2005). The sequences of three independent clones were determined and compared with each other to avoid PCR error and to find conserved mutations. Based on the nucleotide sequence data of all clones sequenced in this study and the data obtained from the O cells (Ikeda et al., 2005), we constructed a phylogenetic tree for the HCV RNAs sequenced (10,972 nucleotides of HCV 5′-UTR to NS5B). The result (Fig. 2D) revealed that the three clones derived from each cell line were mostly clustered and located at similar genetic distances from the origin (ON/C-5B), although O-3 and OB-3 were not clustered completely in the expected positions, suggesting that O ~ OE are independent cell lines. In our sequence analysis, the K1609E mutation found in the O cells was not detected in the OA, OB, OD, and OE cells. However, instead of the K1609E mutation, each cell line possessed a cell line-specific conserved mutation in the NS3 protease region (Table 1). The E1202G, P1115L, Q1112R, and P1115L mutations in the NS3 protease region were detected in the OA, OB, OD, and OE cells, respectively. These results indicated that K1609E was not a representative mutation in genome-length HCV RNA-replicating in the cells. Although Q1112R, P1115L, and E1202G mutations have been detected in other subgenomic HCV replicons (Blight et al., 2000; Krieger et al., 2001; Lohmann et al., 2003), E1202G mutation seems to have little impact on adaptive mutations (Lohmann et al., 2003) and there is no information on whether or not Q1112R and P1115L are adaptive mutations. Since these mutations were detected as cell line-specific conserved NS3 mutations, we estimated that these NS3 mutations are required for genome-length HCV RNA replication. However, we estimated that the D2415G mutation (the carboxyl region of NS5A) detected in the OA cells is not an adaptive mutation, because this is a naturally observed aa substitution (Murphy et al., 2002; Tanaka et al., 1992). In addition, none of the conserved mutations in the upstream of the NS3 region were detected in the OA, OB, and OD cells or in the O cells, although three conserved mutations (I258K and Y361H in E1 and M939V in NS2) were detected in the OE cells (Table 1). Therefore, we focused on the NS3 mutations found in this analysis for further analyses described below.

3.3. Adaptive mutations found in the NS3 region are required for the robust replication of genome-length HCV RNA

To clarify whether or not conserved NS3 mutations (Q1112R, P1115L, E1202G) are adaptive mutations as are the K1609E mutation, we first carried out qualitative analysis regarding the effects of these mutations in ON/C-5B RNA on the efficiency of colony formation (ECF). The effect of the K1609E mutation derived from O cells was also examined for the comparison. We introduced ON/C-5B RNA with a single NS3 mutation into sOc and Oc cells. Since our previous study (Ikeda et al., 2005) indicated that Oc cells possessed overwhelming advantages in the replication of genome-length HCV RNA, one-twentieth of the ON/C-5B RNA used for sOc cells was used for Oc cells. The results revealed that the NS3 mutated RNA-introduced sOc and Oc cells produced a number of G418-resistant colonies, as did those in K1609E mutation-introduced cells, although no and a few G418-resistant colonies were obtained in the original ON/C-5B RNA-introduced sOc and Oc cells, respectively (Fig. 3). Although the K1609E or E1202G mutation was found in the sOc-derived O or OA cells, the effect of the K1609E or E1202G mutation was not different from that of the Q1112R or P1115L mutation found in the Oc-derived OB, OD, or OE cells. This result indicated that the effects of these mutations are not dependent on their cell origins, and that the Q1112R, P1115L, and E1202G mutations also worked as cell culture-adaptive mutations, as did the K1609E mutation in both sOc and Oc cells. Furthermore, these results indicated again that Oc cells are superior to sOc cells regarding the intracellular replication of genome-length HCV RNA, supporting the previous suggestion (Ikeda et al., 2005) that the cell backgrounds for the potentials of the RNA replication are rather different between Oc and sOc cells.

We next performed quantitative analysis whether or not the effects of these adaptive mutations on ECF are correlated with the effects in early events after RNA transfection into the cells, because of the possibility that additional adaptive mutations

Table 1
Summary of genetic analysis of HCV RNAs derived from O, OA, OB, OD, and OE cells

Cell	Cell background	Size (Nts)	Clone number sequenced	Conserved mutations
O	sOc	10972	3	K1609E (NS3)
OA	sOc	10972	3	E1202G (NS3) D2415G (NS 5A)
OB	Oc	10972	3	P1115L (NS3)
OD	Oc	10972	3	Q1112R (NS3)
OE	Oc	10972	3	I258K (E1) Y361H (E1) M939V (NS2) P1115L (NS3)

Only amino acid positions substituted in all three clones are indicated as the conserved mutations.

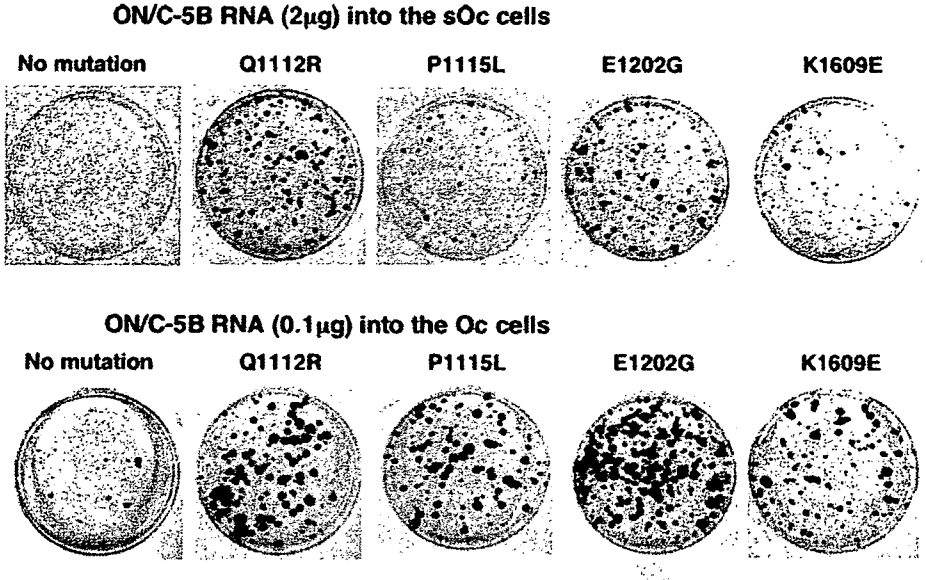

Fig. 3. Adaptive mutations found in the NS3 region show the different ECFs between the sOc and Oc cells. ON/C-5B RNA or ON/C-5B RNA with an additional NS3 mutation was transfected into the sOc cells (2 μg RNA per 10 cm dish; top panel) and the Oc cells (0.1 μg RNA per 10 cm dish; bottom panel). The panels show G418-resistant colonies that were stained with Coomassie brilliant blue at 3 weeks after RNA transfection (Naganuma et al., 2004).

occur during G418 selection for 3 weeks. For the development of a transient replication assay using the RL reporter gene, we first constructed pOR/C-5B from pON/C-5B by replacing the RL and *Neo*^{R} genes (Fig. 1). Next, we made OR/C-5B RNA with the Q1112R, P1115L, E1202G, or K1609E mutation, and then introduced these RNAs into the Oc cells by electroporation. OR/C-5B RNA with dGDD was used as a negative control. The results revealed that the luciferase activity increased in a time-dependent manner when OR/C-5B RNA with an adaptive NS3 mutation was transfected, whereas the activity decreased with time when OR/C-5B RNA without an adaptive NS3 mutation or with dGDD was transfected (Fig. 4A). These results suggest that genome-length HCV RNA with an adaptive NS3 mutation is efficiently able to replicate immediately after transfection. At 96 h, the luciferase activities in the cases of the adaptive NS3 mutation were approximately twice those at 24 h after RNA transfection, and no significant differences in replication efficiency among the adaptive NS3 mutations were observed (Fig. 4A). In summary, we demonstrated a good correlation between the ECF assay (Fig. 3) and luciferase reporter assay for transient replication (Fig. 4A). Therefore, we conclude that Q1112R, P1115L, E1202G, and K1609E function as cell culture-adaptive mutations, and that at least one of them is required for efficient replication of genome-length HCV RNA.

3.4. Every combination of adaptive NS3 mutations in the Oc cells caused more effective genome-length HCV RNA replication than any single adaptive NS3 mutation

According to previous reports using subgenomic HCV replicons, some combinations of adaptive mutations drastically enhance ECF (Krieger et al., 2001; Lohmann et al., 2001, 2003). However, some combinations of adaptive mutations reduced ECF drastically (Lohmann et al., 2001, 2003), suggesting that some adaptive mutations are not compatible. To examine whether or not such conflicting effects of adaptive mutations are observed in genome-length HCV RNA replication, we tested the effects of combining the adaptive NS3 mutations identified in this study, using the luciferase reporter assay for transient replication. We prepared six kinds of OR/C-5B RNA with double adaptive NS3 mutations (i.e., Q1112R and P1115L), and then introduced these RNAs into the Oc cells by electroporation. OR/C-5B RNA with the K1609E mutation was used as a representative of a single adaptive NS3 mutation, and OR/C-5B RNA with dGDD was used as a negative control. The results revealed that the luciferase activities in every combination of adaptive NS3 mutations were remarkably increased, to approximately four- to nine-fold at 96 h, in comparison with the activities at 24 h after RNA transfection, although the enhancement of the luciferase activity by the K1609E mutation was only approximately two-fold (Fig. 4B). The combination of Q1112R and K1609E mutations was the most effective in the Oc cells, followed by that of Q1112R and P1115L mutations. These results suggest that all adaptive NS3 mutations identified in this study are compatible for genome-length HCV RNA replication. It is noteworthy that Q1112R and P1115L mutations are compatible, regardless of very near localization in the NS3 protease.

3.5. Specific combination of adaptive NS3 mutations drastically enhanced genome-length HCV RNA replication, regardless of cell lines

Although we found that every combination of adaptive NS3 mutations caused more effective genome-length HCV RNA replication than any single adaptive NS3 mutation and that some combinations of the mutations drastically enhanced RNA replication (Fig. 4B), the possibility remains that these findings are due to cell clonality, because a cloned Oc cell line was used

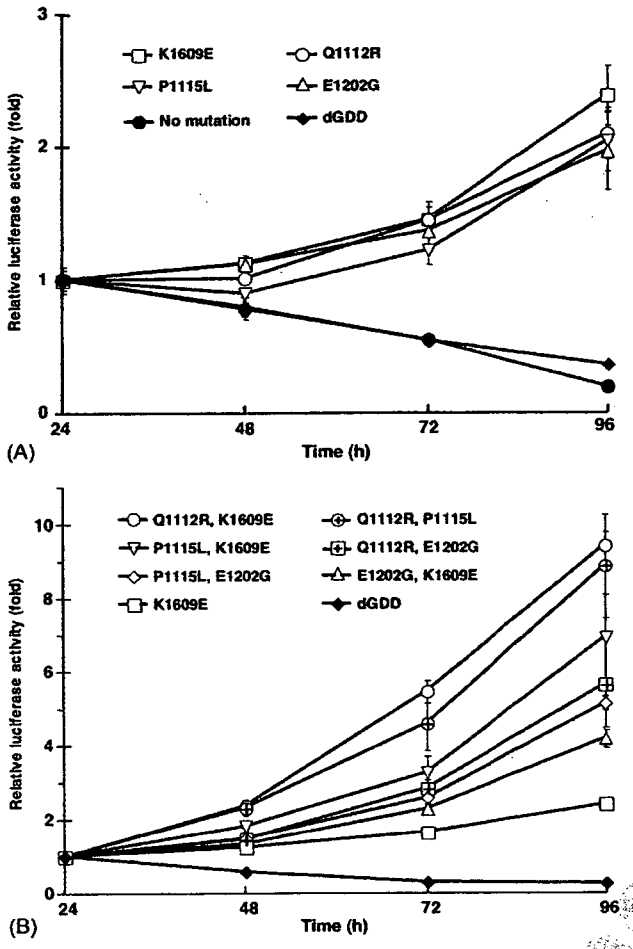

Fig. 4. Transient replication assay of genome-length HCV RNA. (A) Effects of adaptive NS3 mutations on transient replication of genome-length HCV RNA. OR/C-5B RNA or OR/C-5B RNA with an additional mutation was transfected into the Oc cells, and luciferase activity was determined in cell lysates that were prepared at given time points post-transfection. Values for each time point correspond to the mean and the error range of quadruplicate results. Note that, owing to the slightness of the variations, error bars are in some cases not viable in the graph. Values are corrected for transfection efficiency as determined by measuring the luciferase activity 24 h after transfection. dGDD indicates the deletion of the GDD motif in the NS5B polymerase, and the genome-length HCV RNA with dGDD was used as a negative control. (B) Combination effects of adaptive NS3 mutations on transient replication of genome-length HCV RNA. OR/C-5B RNAs with various combinations of adaptive NS3 mutations were transfected into the Oc cells, and luciferase activity was determined in cell lysates that were prepared at given time points post-transfection, as shown in (A). For a comparison of the results, OR/C-5B RNA with K1609E was used as a representative of a single adaptive mutation.

for the analysis. To check this possibility, we tested the effects of combining adaptive NS3 mutations in the cured OAc, OBc, ODc, and OEc cells, using the transient replication assay as described above. sOc cells, which are rather inferior to the Oc cells in RNA replication (Ikeda et al., 2005; Fig. 3), were also used for the analysis. Interestingly, in the OAc, OBc, ODc, and OEc cells also, the results were similar to those obtained in the Oc cells. The combination of Q1112R and K1609E mutations or Q1112R and P1115L mutations was the most effective on the genome-length HCV RNA replication, although the combination of P1115L and K1609E mutations or E1202G and K1609E mutations was not effective in ODc cells (Fig. 5). These results suggest that the NS3 with specific adaptive mutations is the primary determinant of the replication level of genome-length HCV RNA, regardless of cell lines. In addition, we found that OEc cells possessed the best environment for RNA replication among examined cell lines, by demonstrating that the luciferase activity in the combination of Q1112R and K1609E mutations was approximately 20-fold higher at 96 h than that at 24 h after RNA transfection (Fig. 5). On the other hand, we observed that most combinations of adaptive mutations in the sOc cells did not enhance RNA replication, although luciferase activity was enhanced approximately two-fold in the combination of Q1112R and P1115L only (Fig. 5). These results suggest that the cellular environment is also involved in the efficient replication of genome-length HCV RNA.

4. Discussion

In this study, we established four kinds of genome-length HCV RNA (O strain of genotype 1b) replicating cell lines (OA, OB, OD, and OE), which were independent from the O cell line established previously (Ikeda et al., 2005). We also found several cell culture-adaptive NS3 mutations required for the replication of genome-length HCV RNA. We further found that specific combinations of these adaptive mutations remarkably enhanced the efficiency of the RNA replication, regardless of the cell lines obtained.

To establish genome-length HCV RNA-replicating cell lines, we introduced ON/C-5B RNA with the S2200R mutation (NS5A), which was identified as the adaptive mutation for the sO replicon, into two types (sOc and Oc) of cured cells. Since the ECF of the Oc cells was higher than that of the parental sOc cells (Ikeda et al., 2005), the Oc cells were also used to facilitate the establishment of genome-length HCV RNA-replicating cell lines. We initially estimated that adaptive mutations other than K1609E (NS3 helicase region) found in the O cells would be obtained from the sOc-derived OA cell line, and that the K1609E mutation would be obtained mainly from the Oc-derived OB, OD, and OE cell lines. Although a new E1202G adaptive mutation was obtained from the sOc-derived OA cells, the K1609E mutation was not obtained from the Oc-derived OB, OD, and OE cells. Instead of the K1609E mutation, the P1115L adaptive mutation (NS3 protease region) was obtained from the OB and OE cells, and the Q1112R adaptive mutation (NS3 protease region) was obtained from the OD cells. The ECF assay and transient replication assay showed that these adaptive mutations possessed similar potentials of genome-length HCV RNA replication in the Oc cells. These results suggest that the K1609E mutation is only one of the adaptive mutations that function in the Oc cells, and suggest that the combination of an NS3 mutation (Q1112R, P1115L, E1202G, or K1609E) with the NS5A mutation (S2200R) is required for efficient replication of genome-length HCV RNA, although only the S2200R mutation is enough to efficiently replicate the subgenomic sO replicon (Kato and Sugiyama et al., 2003). Therefore, our findings suggest that viral factors, which are not required for the robust

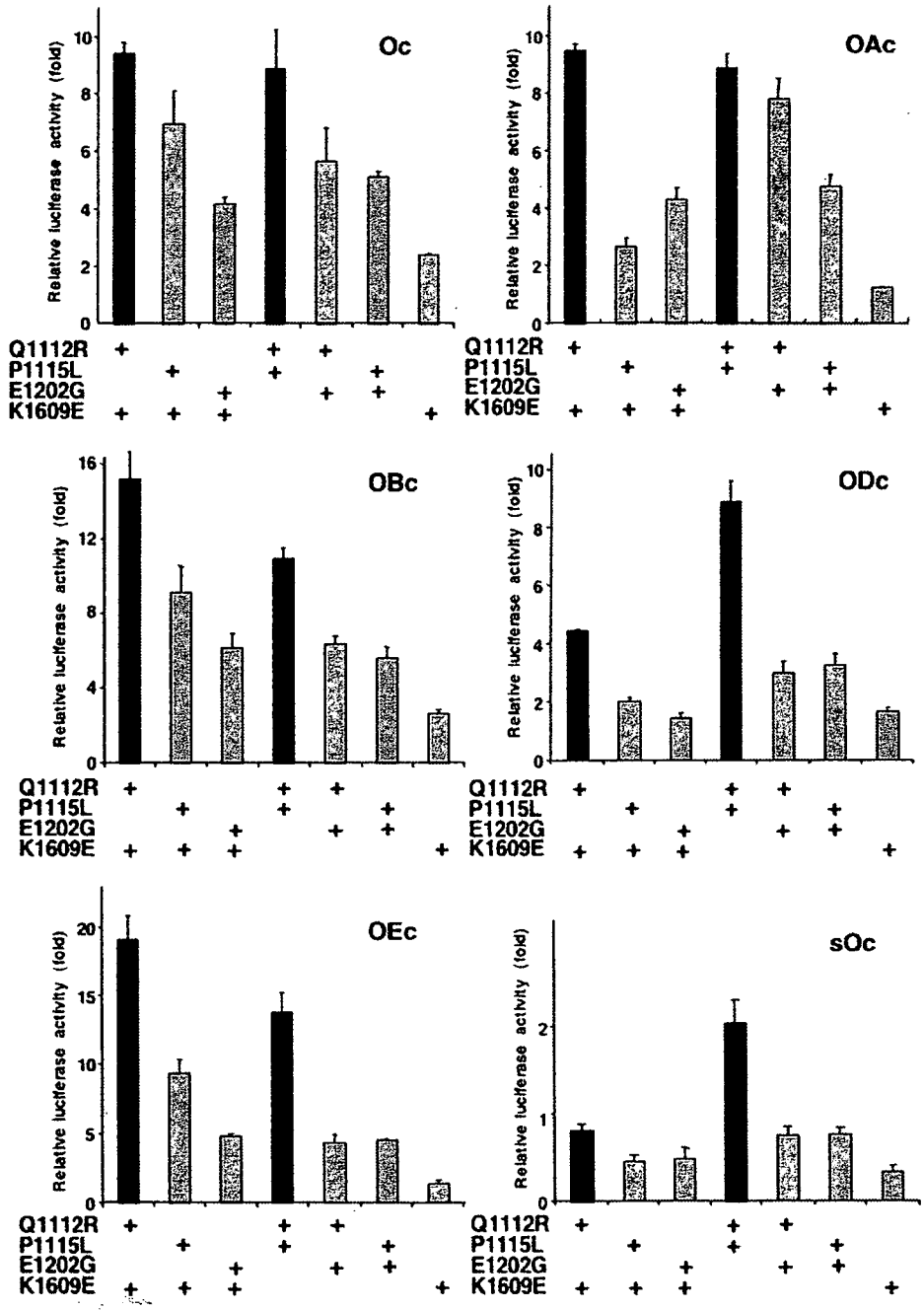

Fig. 5. Effects of combining adaptive NS3 mutations on transient genome-length HCV RNA replication in various cured cells. OR/C-5B RNAs with various combinations of adaptive NS3 mutations were transfected into various cured cells (Oc, OAc, OBc, ODc, OEc, and sOc cells), and luciferase activity was determined in cell lysates that were prepared at 96 h post-transfection, as shown in Fig. 4. Values are corrected for transfection efficiency as determined by measuring the luciferase activity 24 h after transfection.

replication of a subgenomic HCV replicon, are required for the robust replications of genome-length HCV RNA.

To date, it has been believed that cell culture-adaptive mutations that enhance HCV RNA replication do not exist in HCV-infected patients (Bartenschlager, 2005). However, Sarrazin et al. (2005) recently reported the existence of adaptive NS3 mutations in 5 of 26 HCV-infected patients. In that study, it is noteworthy that mutations (P1112R and P1115G) in positions 1112 and 1115 have been found, although Q1112R and P1115L have not been detected, and that specific adaptive mutations have been associated with a slower initial decrease in HCV RNA concentrations during IFN-α-based antiviral therapy (Sarrazin et al., 2005). Furthermore, a search of the Hepatitis Virus Database (Nagoya City University, Japan) found Q1112R, P1115L, and E1202G in the HCV sequences (accession nos. AY460204, D84262, and AF011751, respectively) derived from HCV-infected patients. Therefore, some of the cell culture-adaptive mutations may not be artificial mutations

but may reflect some phenomena that HCV-infected patients undergo.

Although adaptive NS3 mutations found in this study were the same as those detected in subgenomic HCV replicons derived from different HCV strains (Blight et al., 2000; Kishine et al., 2002; Krieger et al., 2001; Lohmann et al., 2001, 2003), the impacts of these mutations in subgenomic HCV replicons seem to be small. The impacts of E1202G and K1609E on ECF assay and transient replication assay, respectively, were only about four- and two-fold that of the wild-type subgenomic HCV replicon (Lohmann et al., 2001, 2003), and information regarding Q1112R and P1115L mutations has yet to be reported. However, we observed that Q1112R, P1115L, E1202G, and K1609E mutations remarkably enhanced the efficiency of genome-length HCV RNA replication in both ECF and transient replication assay (Figs. 3 and 4). The discrepancy in the results might be due to the differences in subgenomic and genomic lengths of HCV RNA, in HCV strains, or in host cell lines used. Recently, we showed time-dependent genetic mutations of subgenomic HCV replicons and time-dependent expansions of their genetic diversities in long-term culture (at least 1 year) of two cell lines harboring subgenomic HCV replicons (1B-1 and O strains) (Kato et al., 2005). In that study, we observed that the expansion of the replicons' genetic diversity was associated with the enhancement of RNA replication. It is noteworthy that the P1115L mutation has been detected as a conserved mutation after 6 months in cell culture of the 1B-1-derived replicon, although this mutation's contribution to the replication is not clear (Kato et al., 2005). Genetic analysis of HCV RNAs in long-term cultures of O ~ OE cells will provide useful information regarding the genetic advantages of adaptive mutations found in the NS3 region. For such analysis, long-term culture (at least 1 year) of O ~ OE cells is in progress.

From the analyses using subgenomic HCV replicons to date, the center of NS5A has been thought to represent a hot spot for cell culture-adaptive mutations, because most mutations are found in this region. Interestingly, adaptive mutations often affect serine residues involved in hyperphosphorylation of NS5A. Although the HCV-O-derived sO replicon also possesses a unique S2200R adaptive mutation in the center of NS5A, the serine residue at position 2200 is not thought to be involved in the hyperphosphorylation of NS5A (Tanji et al., 1995). To examine whether or not S2200R mutation is required for efficient replication of genome-length HCV RNA, we tested the effect of the S2200R mutation on RNA replication by the introduction of OR/C-5B RNA with Q1112R and K1609E, in which the arginine residue in position 2200 was restored to serine residue, into Oc cells. The results revealed that the replication of genome-length HCV RNA was abolished with the restoration only in position 2200 (data not shown), suggesting that the S2200R mutation plays an important key role in HCV RNA replication in HuH-7-derived cells. However, the mechanism underlying the mutations found in NS3 causes the replication of genome-length HCV RNA is unknown, as is the mechanism underlying the great enhancement of replication by the combination of NS3 mutations. One possibility is that the NS3 mutations found in this study are able to drastically enhance the protease or helicase activity of NS3. To evaluate this possibility, further experiments using the quantitative system that measures the NS3 protease or helicase activity will be needed.

The relation between the combination of adaptive NS3 mutations and the cloned cell lines is interesting. From information obtained in previous studies (Lohmann et al., 2003; Ikeda et al., 2005) and the present study, it clearly appeared that both viral and cellular factors contributed to HCV RNA replication in cell culture. For the replication of genome-length HCV RNA, we showed that adaptive NS3 mutations were viral factors and that the differences between sOc and Oc cells were cellular factors (Fig. 3). However, our results revealed that specific combinations of adaptive NS3 mutations (Q1112R and K1609E, or Q1112R and P1115L) were superior to the other combinations in all Oc, OAc, OBc, ODc, and OEc cell lines examined. In even sOc cells, the combination of Q1112R and P1115L, but not the combination of Q1112R and K1609E, was superior to the other combinations. These findings suggest that the effect of NS3 possessing a specific combination of mutations is superior to that of the host cell clonality. Recently, Yi et al. (2006) reported the production of infectious genotype 1a HCV in the cells transfected with genome-length HCV RNA (H77-S) possessing five adaptive mutations (two in NS3, one in NS4A, and two in NS5A), suggesting that robust replication of HCV RNA is also necessary for the production of infectious viruses (Yi et al., 2006). Therefore, identification of the best combination of adaptive mutations for efficient RNA replication may be useful in the development of a system to produce infectious genotype 1b HCV, and for understanding the HCV replication mechanism.

Acknowledgments

We thank T. Nakamura and A. Morishita for their technical assistance. This work was supported by a grant-in-aid for the third-term comprehensive 10-year strategy for cancer control and by a grant-in-aid for research on hepatitis, both from the Ministry of Health, Labor, and Welfare of Japan. K.A. was supported by a Research Fellowship from the Japan Society for the Promotion of Science (JSPS) for Young Scientists.

References

Abe, K., Ikeda, M., Dansako, H., Naka, K., Shimotohno, K., Kato, N., 2005. cDNA microarray analysis to compare HCV subgenomic replicon cells with their cured cells. Virus Res. 107, 73–81.

Ali, S., Pellerin, C., Lamarre, D., Kukolj, G., 2004. Hepatitis C virus subgenomic replicons in the human embryonic kidney 293 cell line. J. Virol. 78, 491–501.

Appel, N., Pietschmann, T., Bartenschlager, R., 2005. Mutational analysis of hepatitis C virus nonstructural protein 5A: potential role of differential phosphorylation in RNA replication and identification of a genetically flexible domain. J. Virol. 79, 3187–3194.

Bartenschlager, R., 2002. Hepatitis C virus replicons: potential role for drug development. Nat. Rev. Drug Discov. 1, 911–996.

Bartenschlager, R., 2005. The hepatitis C virus replicon system: from basic research to clinical application. J. Hepatol. 43, 210–216.

Bartenschlager, R., Lohmann, V., 2000. Replication of hepatitis C virus. J. Gen. Virol. 81, 1631–1648.

Blight, K.J., Kolykhalov, A.A., Rice, C.M., 2000. Efficient initiation of HCV RNA replication in cell culture. Science 290, 1972–1974.

Blight, K.J., McKeating, J.A., Rice, C.M., 2002. Highly permissive cell lines for subgenomic and genomic hepatitis C virus RNA replication. J. Virol. 76, 13001–13014.

Blight, K.J., McKeating, J.A., Marcotrigiano, J., Rice, C.M., 2003. Efficient replication of hepatitis C virus genotype 1a RNAs in cell culture. J. Virol. 77, 3181–3190.

Date, T., Kato, T., Miyamoto, M., Zhao, Z., Yasui, K., Mizokami, M., Wakita, T., 2004. Genotype 2a hepatitis C virus subgenomic replicon can replicate in HepG2 and IMY-N9 cells. J. Biol. Chem. 279, 22371–22376.

Grobler, J.A., Markel, E.J., Fay, J.F., Graham, D.J., Simcoe, A.L., Ludmerer, S.W., Murray, E.M., Migliaccio, G., Flores, O.A., 2003. Identification of a key determinant of hepatitis C virus cell culture adaptation in domain II of NS3 helicase. J. Biol. Chem. 278, 16741–16746.

Hijikata, M., Kato, N., Ootsuyama, Y., Nakagawa, M., Shimotohno, K., 1991. Gene mapping of the putative structural region of the hepatitis C virus genome by in vitro processing analysis. Proc. Natl. Acad. Sci. U.S.A. 88, 5547–5551.

Hijikata, M., Mizushima, H., Tanji, Y., Komoda, Y., Hirowatari, Y., Akagi, T., Kato, N., Kimura, K., Shimotohno, K., 1993. Proteolytic processing and membrane association of putative nonstructural proteins of hepatitis C virus. Proc. Natl. Acad. Sci. U.S.A. 90, 10773–10777.

Ikeda, M., Yi, M., Li, K., Lemon, S.M., 2002. Selectable subgenomic and genome-length dicistronic RNAs derived from an infectious molecular clone of the HCV-N strain of hepatitis C virus replicate efficiently in cultured Huh7 cells. J. Virol. 76, 2997–3006.

Ikeda, M., Abe, K., Dansako, H., Nakamura, T., Naka, K., Kato, N., 2005. Efficient replication of a full-length hepatitis C virus genome, strain O, in cell culture, and development of a luciferase reporter system. Biochem. Biophys. Res. Commun. 329, 1350–1359.

Kato, N., 2001. Molecular virology of hepatitis C virus. Acta Med. Okayama 55, 133–159.

Kato, N., Shimotohno, K., 2000. Systems to culture hepatitis C virus. Curr. Top. Microbiol. Immunol. 242, 261–278.

Kato, N., Hijikata, M., Ootsuyama, Y., Nakagawa, M., Ohkoshi, S., Sugimura, T., Shimotohno, K., 1990. Molecular cloning of the human hepatitis C virus genome from Japanese patients with non-A, non-B hepatitis. Proc. Natl. Acad. Sci. U.S.A. 87, 9524–9528.

Kato, N., Sugiyama, K., Namba, K., Dansako, H., Nakamura, T., Takami, M., Naka, K., Nozaki, A., Shimotohno, K., 2003. Establishment of a hepatitis C virus subgenomic replicon derived from human hepatocytes infected in vitro. Biochem. Biophys. Res. Commun. 306, 756–766.

Kato, T., Date, T., Miyamoto, M., Furusaka, A., Tokushige, K., Mizokami, M., Wakita, T., 2003. Efficient replication of the genotype 2a hepatitis C virus subgenomic replicon. Gastroenterology 125, 1808–1817.

Kato, N., Nakamura, T., Dansako, H., Namba, K., Abe, K., Nozaki, A., Naka, K., Ikeda, M., Shimotohno, K., 2005. Genetic variation and dynamics of hepatitis C virus replicons in long-term cell culture. J. Gen. Virol. 86, 645–656.

Kishine, H., Sugiyama, K., Hijikata, M., Kato, N., Takahashi, H., Noshi, T., Nio, Y., Hosaka, M., Miyanari, Y., Shimotohno, K., 2002. Subgenomic replicon derived from a cell line infected with the hepatitis C virus. Biochem. Biophys. Res. Commun. 293, 993–999.

Krieger, N., Lohmann, V., Bartenschlager, R., 2001. Enhancement of hepatitis C virus RNA replication by cell culture-adaptive mutations. J. Virol. 75, 4614–4624.

Lindenbach, B.D., Rice, C.M., 2005. Unravelling hepatitis C virus replication from genome to function. Nature 436, 933–938.

Lindenbach, B.D., Evans, M.J., Syder, A.J., Wolk, B., Tellinghuisen, T.L., Liu, C.C., Maruyama, T., Hynes, R.O., Burton, D.R., McKeating, J.A., Rice, C.M., 2005. Complete replication of hepatitis C virus in cell culture. Science 309, 623–626.

Lohmann, V., Korner, F., Koch, J., Herian, U., Theilmann, L., Bartenschlager, R., 1999. Replication of subgenomic hepatitis C virus RNAs in a hepatoma cell line. Science 285, 110–113.

Lohmann, V., Korner, F., Dobierzewska, A., Bartenschlager, R., 2001. Mutations in hepatitis C virus RNAs conferring cell culture adaptation. J. Virol. 75, 1437–1449.

Lohmann, V., Hoffmann, S., Herian, U., Penin, F., Bartenschlager, R., 2003. Viral and cellular determinants of hepatitis C virus RNA replication in cell culture. J. Virol. 77, 3007–3019.

Murphy, M.D., Rosen, H.R., Marousek, G.I., Chou, S., 2002. Analysis of sequence configurations of the ISDR, PKR-binding domain, and V3 region as predictors of response to induction interferon-alpha and ribavirin therapy in chronic hepatitis C infection. Digest. Dis. Sci. 47, 1195–1205.

Naganuma, A., Nozaki, A., Tanaka, T., Sugiyama, K., Takagi, H., Mori, M., Shimotohno, K., Kato, N., 2000. Activation of the interferon-inducible 2′-5′-oligoadenylate synthetase gene by hepatitis C virus core protein. J. Virol. 74, 8744–8750.

Naganuma, A., Dansako, H., Nakamura, T., Nozaki, A., Kato, N., 2004. Disturbance of the DNA repair system by HCV core protein. Cancer Res. 64, 1307–1314.

Naka, K., Takemoto, K., Abe, K., Dansako, H., Ikeda, M., Shimotohno, K., Kato, N., 2005. Interferon resistance of hepatitis C virus replicon-harbouring cells is caused by functional disruption of type I interferon receptors. J. Gen. Virol. 86, 2787–2792.

Pietschmann, T., Lohmann, V., Kaul, A., Krieger, N., Rinck, G., Rutter, G., Strand, D., Bartenschlager, R., 2002. Persistent and transient replication of full-length hepatitis C virus genomes in cell culture. J. Virol. 76, 4008–4021.

Sarrazin, C., Mihm, U., Herrmann, E., Welsch, C., Albrecht, M., Sarrazin, U., Traver, S., Lengauer, T., Zeuzem, S., 2005. Clinical significance of in vitro replication-enhancing mutations of the hepatitis C virus (HCV) replicon in patients with chronic HCV infection. J. Infect. Dis. 192, 1710–1719.

Tanaka, T., Kato, N., Nakagawa, M., Ootsuyama, Y., Cho, M.J., Nakazawa, T., Hijikata, M., Ishimura, Y., Shimotohno, K., 1992. Molecular cloning of hepatitis C virus genome from a single Japanese carrier: sequence variation within the same individual and among infected individuals. Virus Res. 23, 39–53.

Tanaka, T., Kato, N., Cho, M.J., Shimotohno, K., 1995. A novel sequence found at the 3′ terminus of hepatitis C virus genome. Biochem. Biophys. Res. Commun. 215, 744–749.

Tanji, Y., Kaneko, T., Satoh, S., Shimotohno, K., 1995. Phosphorylation of hepatitis C virus-encoded nonstructural protein NS5A. J. Virol. 69, 3980–3986.

Thomas, D.L., 2000. Hepatitis C epidemiology. Curr. Top. Microbiol. Immunol. 242, 25–41.

Wakita, T., Pietschmann, T., Kato, T., Date, T., Miyamoto, M., Zhao, Z., Murthy, K., Habermann, A., Krausslich, H.G., Mizokami, M., Bartenschlager, R., Liang, T.J., 2005. Production of infectious hepatitis C virus in tissue culture from a cloned viral genome. Nat. Med. 11, 791–796.

Yi, M., Lemon, S.M., 2004. Adaptive mutations producing efficient replication of genotype 1a hepatitis C virus RNA in normal Huh7 cells. J. Virol. 78, 7904–7915.

Yi, M., Villanueva, R.A., Thomas, D.L., Wakita, T., Lemon, S.M., 2006. Production of infectious genotype 1a hepatitis C virus (Hutchinson strain) in cultured human hepatoma cells. Proc. Natl. Acad. Sci. U.S.A. 103, 2310–2315.

Zhong, J., Gastaminza, P., Cheng, G., Kapadia, S., Kato, T., Burton, D.R., Wieland, S.F., Uprichard, S.L., Wakita, T., Chisari, F.V., 2005. Robust hepatitis C virus infection in vitro. Proc. Natl. Acad. Sci. U.S.A. 102, 9294–9299.

Zhu, Q., Guo, J.T., Seeger, C., 2003. Replication of hepatitis C virus subgenomes in nonhepatic epithelial and mouse hepatoma cells. J. Virol. 77, 9204–9210.

Original Paper

Intervirology

Intervirology 2007;50:394–401
DOI: 10.1159/000110651

Received: April 23, 2007
Accepted after revision: August 7, 2007
Published online: October 31, 2007

Type B Fulminant Hepatitis Is Closely Associated with a Highly Mutated Hepatitis B Virus Strain

Aimi Kanada[a] Tetsuo Takehara[a] Kazuyoshi Ohkawa[a, b] Tomohide Tatsumi[a] Ryotaro Sakamori[a] Shinjiro Yamaguchi[a] Akio Uemura[a] Keisuke Kohga[a] Akira Sasakawa[a] Hayato Hikita[a] Taizo Hijioka[c] Kazuhiro Katayama[d] Matsuo Deguchi[e] Masanori Kagita[e] Tatsuya Kanto[a, b] Naoki Hiramatsu[a] Norio Hayashi[a]

[a]Department of Gastroenterology and Hepatology, and [b]Department of Dendritic Cellular Research and Clinical Application, Osaka University Graduate School of Medicine, Suita, [c]Department of Gastroenterology, National Hospital Organization Osaka Minami National Hospital, Kawachinagano, [d]Department of Internal Medicine, Osaka Koseinenkin Hospital, Osaka, and [e]The Laboratory for Clinical Investigation, Osaka University Hospital, Suita, Japan

Key Words
Hepatitis B virus · Type B acute self-limited hepatitis · Type B fulminant hepatitis · Hepatitis B virus mutation · Full-length hepatitis B virus nucleotide sequencing

Abstract
Objective: Genome-wide sequences of hepatitis B virus strain associated with type B fulminant hepatitis have not been compared with those of acute self-limited hepatitis. We carried out full-length sequencing analysis of viral strains derived from patients with type B acute liver injury. ***Methods:*** Nine acute self-limited hepatitis and 6 fulminant hepatitis patients were the subjects of this study. Full-length sequencing analysis of viral DNA was done by PCR-direct sequencing. ***Results:*** Higher frequencies in fulminant hepatitis strains compared with acute hepatitis ones were observed in the T1762/A1764 ($p < 0.05$), A1896 ($p = 0.09$) and M1753 (M = C or A) ($p = 0.09$) mutations. Viruses related to fulminant hepatitis possessed the higher number of nucleotide substitutions than those related to acute hepatitis in the whole virus genome ($p < 0.01$) and various regions including preS/S gene ($p < 0.05$), precore/core gene ($p < 0.01$), polymerase gene ($p < 0.05$) and basic core promoter/core upstream regulatory sequence ($p < 0.01$). The high number of nucleotide substitutions in viruses related to fulminant hepatitis was predominantly non-synonymous in the preS/S and precore/core genes. ***Conclusion:*** Development of type B fulminant hepatitis may be associated with a highly mutated hepatitis B virus strain.

Introduction

Hepatitis B virus (HBV) is a double-stranded, circular, hepatotropic DNA virus of approximately 3.2 kb in length and causes both acute and chronic liver diseases. Acute HBV infection results in various liver diseases ranging from acute self-limited hepatitis (AH) to fulminant hepatitis (FH). FH develops in approximately 1% of patients with acute type B liver disease [1]. It is believed that a hyperimmune response to viral antigens and/or enhanced viral replicative activity may be relevant to the development of type B FH.

Processes in HBV replication include a reverse transcription step, and hence, HBV is more susceptible to mutations than other DNA viruses because the viral reverse

KARGER
Fax +41 61 306 12 34
E-Mail karger@karger.ch
www.karger.com

0300–5526/07/0506–0394$23.50/0

Accessible online at:
www.karger.com/int

Norio Hayashi, MD, PhD
Department of Gastroenterology and Hepatology
Osaka University Graduate School of Medicine
Suita 565-0871 (Japan)
Tel. +81 6 6879 3620, Fax +81 6 6879 3629, E-Mail hayashin@gh.med.osaka-u.ac.jp

transcriptase lacks proofreading activity. During the past 15 years, a great number of reports have revealed a relationship between the particular mutations within the HBV genome and various clinical manifestations during the course of HBV infection. Mutations within the precore and basic core promoter (BCP) regions have been documented with regard to comparison between AH and FH. The A1896 mutation, which produces the in-frame stop codon in the distal precore gene and results in the incapability to synthesize hepatitis B e antigen (HBeAg) [2], has been shown to be more frequently found in viruses from FH patients than in those from AH ones [3, 4]. Patients with FH have also been reported to possess the virus with T1762/A1764 double mutation in the BCP, which is another type of mutation associated with the HBeAg-negative phenotype through reduced synthesis of precore mRNA [5, 6], more frequently than those with AH [7]. In addition, more frequent detection of the V1753 or V1754 (V = C, G or A) mutation has been reported in the BCP in the FH-related virus than in the AH-related one [8]. The presence of these mutation hotspots associated with FH in the precore and BCP regions of HBV has recently been verified in a large-scale study including approximately 300 patients with acute HBV infection [9]. However, genomic changes occurring in other regions of HBV associated with the development of FH have not been extensively studied.

There have been several reports that have determined the full-length nucleotide sequences of the HBV DNA strains in a single patient or a limited number of patients with FH [10–15]. It has been shown that most of these HBV strains revealed considerable differences in nucleotide and amino acid sequences, compared with the previously reported consensus viral strain [10–15]. However, these studies have analyzed the full-length viral sequences only for the FH-related strain and did not directly compare the viral sequences derived from AH and FH patients. Thus, peculiarities over the entire HBV genome have not been clarified in strains derived from FH patients in comparison to those derived from AH patients.

To better understand the differences between AH and FH strains, we conducted sequencing analysis of full-length HBV DNA derived from patients with HBV-related acute liver injury and compared the nucleotide sequences between viral strains from AH and FH patients.

Patients and Methods

Patients

The subjects in this study were 15 consecutive Japanese patients with HBV-related acute liver injury, who had been admitted to Osaka University Hospital, Osaka Koseinenkin Hospital and National Hospital Organization Osaka Minami National Hospital. They were 12 males and 3 females, ranging in age from 17 to 72 (median 49) years. None of them had been previously found to have abnormal liver function test results. All of them displayed a sudden onset of the clinical signs of acute liver injury. Of the 15 patients, 6 were diagnosed as FH, because they fulfilled the criteria of fulminant hepatic failure as proposed by Trey and Davidson [16] with the minor modifications of the Inuyama Symposium 1981 (Aichi, Japan); i.e., a prothrombin time ≤40% of control and coma ≥ grade II having developed within 8 weeks after the onset of illness. The remaining 9 patients showed neither encephalopathy nor coagulopathy and were diagnosed as AH. 13 patients tested positive for the immunoglobulin M antibody to hepatitis B core antigen (IgM anti-HBc) and were considered to be infected with HBV for the first time. The possibility of acute exacerbation from a chronic carrier state of HBV could not be excluded in the remaining 2 patients belonging to the FH group, who were hepatitis B surface antigen (HBsAg)-positive but IgM anti-HBc-negative. All patients tested negative for IgM antibody to hepatitis A virus, and antibodies to hepatitis C and human immunodeficiency viruses. None of them showed evidence of other kinds of liver diseases, such as alcoholic liver disorder, autoimmune hepatitis and drug-induced liver injury. As for the prognosis, 4 FH patients, 1 of whom received living donor transplantation, died of hepatic failure, whereas the remaining 11 patients recovered without transition into chronicity. The patient clinical characteristics are summarized in table 1. There was no significant difference in age, gender ratio, AST, ALT and HBV DNA between the AH and FH patients. Those with FH did have a higher total bilirubin than those with AH (median 9.1 [range 4.9–17.3] mg/dl vs. median 3.0 [range 0.6–6.8] mg/dl, $p < 0.01$). The prothrombin time was lower in patients with FH (median 22 [range 15–31] % of the control) than in those with AH (median 79 [range 45–111]% of the control) ($p < 0.002$). Serum samples from the patients on admission were collected and stored at −80°C until use. Informed consent was obtained from the patient or patient's family member.

HBV Markers

HBsAg, antibody to HBsAg (anti-HBs), HBeAg, and antibody to HBeAg (anti-HBe) were examined by chemiluminescent immunoassay or enzyme immunoassay. IgM anti-HBc was measured by radioimmunoassay. Serum HBV DNA was detected quantitatively by the PCR-based assay (Amplicor HB Monitor, Roche) [17].

PCR Amplification and Direct Sequencing of Full-Length HBV DNA

The predominant nucleotide sequences of full-length HBV DNA in each of the patients were determined by the PCR-direct sequencing method. Briefly, DNA was extracted from serum samples by the standard procedure with Tris-Cl/EDTA/SDS/proteinase K solution. The first round PCR was undertaken using the primers BF1 (5′-CCG GAA AGC TTG AGC TCT TCT TTT TCA CCT CTG CCT AAT CA-3′, nt 1821–1841) and BR1 (5′-CCG GAA AGC TTG AGC TCT TCA AAA AGT TGC ATG GTG CTG G-3′, nt 1825–1806), which were previously designed by Günther et al. [18]. This PCR reaction yielded the amplification of full-length HBV DNA. The second round PCR reactions were done using three sets of primers to obtain mutually overlap-

Table 1. Clinical and virological characteristics of patients with AH and FH

	Age/ gender	AST IU/l	ALT IU/l	Total bilirubin mg/dl	Prothrombin time, %	HBsAg/ anti-HBs	HBeAg/ anti-HBe	IgM anti-HBc	Genotype	T1762/ A1764	A1896	M1753	HBV DNA $\log_{10}$ copies/ml	Liver transplantation	Prognosis
AH patients (n = 9)															
1	47/M	602	1,519	6.4	89	+/–	–/+	+	C2/Ce	–	–	–	3.6	no	surviving
2	37/M	810	4,132	6.8	45	–/+	–/+	+	C2/Ce	+	+	+ (C1753)	3.4	no	surviving
3	43/M	164	587	2.0	61	+/–	–/+	+	C2/Ce	+	–	–	5.8	no	surviving
4	17/F	120	439	0.6	109	+/–	+/+	+	C2/Ce	–	–	–	3.1	no	surviving
5	57/M	902	2,170	1.4	67	+/–	+/–	+	C1/Cs	–	–	–	7.5	no	surviving
6	62/M	140	236	0.9	68	+/–	+/–	+	B2/Ba	–	–	–	>7.6	no	surviving
7	69/M	505	1,905	1.8	111	+/–	–/+	+	C2/Ce	–	–	–	5.8	no	surviving
8	72/M	387	818	0.6	76	+/+	+/–	+	A2/Ae	–	–	–	7.6	no	surviving
9	53/M	806	1,782	6.1	89	+/–	+/–	+	A2/Ae	–	–	–	6.6	no	surviving
FH patients (n = 6)															
10	56/F	1,751	3,561	6.6	15	–/+	+/+	+	C2/Ce	+	–	+ (C1753)	5.3	no	died
11	48/M	9,657	4,825	4.9	31	+/–	+/–	+	C2/Ce	+	+	+ (C1753)	7.0	no	surviving
12	52/M	313	497	11.2	29	+/–	–/+	+	B1/Bj	–	+	–	5.5	no	surviving
13	48/F	1,361	2,872	7.2	22	–/+	–/+	+	B1/Bj	+	+	+ (A1753)	4.6	yes	died
14	49/M	595	1,025	17.3	18	+/–	+/–	–	C2/Ce	+	–	–	5.6	no	died
15	38/M	329	1,127	7.6	15	+/–	–/+	–	C2/Ce	+	+	+ (C1753)	5.9	no	died

ping HBV DNA fragments. The primers were BF1s (5′-TTT TTC ACC TCT GCC TAA TCA-3′, nt 1821–1841), BR5 (5′-AAC TGG AGC CAC CAG CAG GA-3′, nt 74–55), BF4 (5′-GTC ACC ATA TTC TTG GGA AC-3′, nt 2816–2835), BR7 (5′-GGG TTC AAA TGT ATA CCC AA-3′, nt 839–820), BF7 (5′-TAT TGG GGG CCA AGT CTG TA-3′, nt 752–771) and BR1s (5′-AAA AAG TTG CAT GGT GCT GG-3′, nt 1825–1806). All PCR reactions were performed using the Expand High Fidelity PLUS PCR system (Roche). Under this PCR condition, the detection limit of the full-length HBV DNA was approximately 3.0–3.5 $\log_{10}$ copies/ml. After the purification, the BF1s/BR5, BF4/BR7 and BF7/BR1s DNA fragments were subjected to direct sequencing reaction using the BigDye Terminator Version 3.1 Cycle Sequencing Kit and 3100 or 3730 Genetic Analyzer (Applied Biosystems). The cycle sequencing reaction was conducted using primers, BF2 (5′-CAG ACA ACT ATT GTG GTT TC-3′, nt 2191–2210), BF3 (5′-TCT TTA ATC CTG AGT GGC AA-3′, nt 2512–2531), BF5 (5′-AAG AGA CAG TCA TCC TCA GG-3′ nt 3183–3202), BF6 (5′-CCT CCA ATT TGT CCT GGC TA-3′, nt 350–369), BF8 (5′-TTT ACC CCG TTG CCC GGC A-3′, nt 1142–1160), BR2 (5′-CAG AAT AGC TTG CCT GAG TG-3′, nt 2080–2061), BR3 (5′-TTC CCG AGA TTG AGA TCT TC-3′, nt 2440–2421), BR4 (5′-GAC CAA ATG CTC CCG CTC CT-3′, nt 3040–3021) and BR6 (5′-GAG CAG GGG TCC TAG GAA TC-3′ nt 193–174), as well as the above-mentioned primers, BF1s, BF4, BF7, BR5, BR7 and BR1s. The nucleotide sequences of HBV strains determined in this study are shown in the international DNA database with accession numbers of AB300359 to AB300373.

Molecular Genetic Analysis

DNA sequences of the 15 HBV strains derived from the FH and AH patients in this study and 5 representative HBV strains of subgenotypes A2/Ae, B1/Bj, B2/Ba, C1/Cs and C2/Ce (GenBank Accession No. X02763, D00330, D00329, AF223954 and X01587) [19–22] were aligned using the CLUSTALW software. A phylogenetic tree analysis was conducted using Kimura's two-parameter method and the neighbor-joining method [23, 24], and illustrated as a rectangular cladogram using the TreeView software. To quantitatively evaluate the degree of mutation in each of the HBV strains obtained in this study, the number of nucleotide substitutions per site (evolutional distance) was calculated in comparison with the reference HBV strain using Kimura's two-parameter method [23]. The Nei-Gojobori's method [25] with Jukes-Cantor's correction was also used to calculate the numbers of synonymous (silent) substitutions per synonymous site (d_S) and non-synonymous (amino acid-substituting) substitutions per non-synonymous site (d_N) between each HBV strain and the reference strain. In the present study, the above-mentioned HBV strains, X02763, D00330, D00329, AF223954 and X01587 [19–22], of subgenotypes A2/Ae, B1/Bj, B2/Ba, C1/Cs and C2/Ce were used as the references to standardize the value of the number of nucleotide substitutions in different subgenotypes of HBV strains. These analyses were conducted at the homepage of the DNA Data Bank of Japan (http://www.ddbj.nig.ac.jp) or using MEGA version 3.1 software [26].

Statistical Analysis

Mann-Whitney's non-parametric U test and Fisher's exact probability test were used for the group comparison. A p value < 0.05 was considered to be statistically significant.

Results

The nucleotide sequences of full-length HBV DNA derived from the 15 patients with AH and FH were 3158–3227 bp in length. Figure 1 represents the result of the phylogenetic tree analysis including the 15 HBV strains

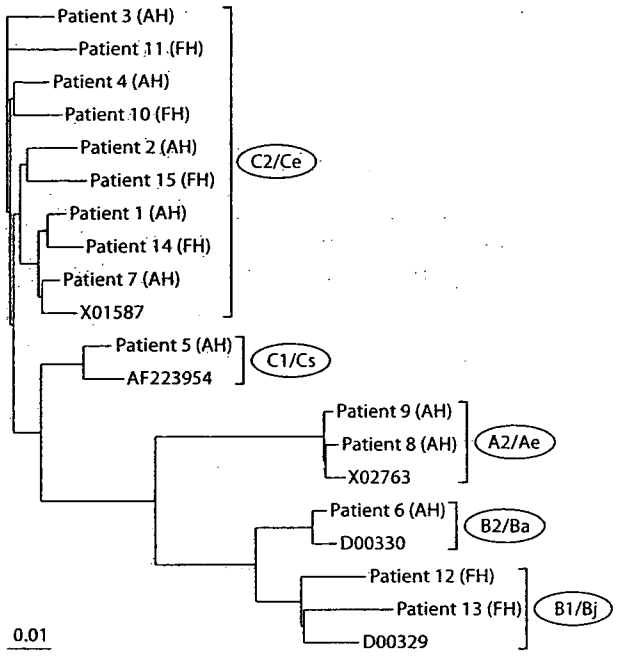

Fig. 1. Phylogenetic tree analysis of 15 HBV strains derived from the AH and FH patients and 5 representative HBV strains of subgenotypes A2/Ae, B1/Bj, B2/Ba, C1/Cs and C2/Ce.

obtained in this study and five representative (reference) HBV strains of subgenotypes A2/Ae, B1/Bj, B2/Ba, C1/Cs and C2/Ce. Among the 15 strains determined in this study, nine from 5 AH and 4 FH patients belonged to subgenotype C2/Ce, the most prevalent type in Japan. There were two subgenotype A2/Ae strains from AH patients, two subgenotype B1/Bj strains from FH patients, one subgenotype B2/Ba strain from an AH patient and one subgenotype C1/Cs strain from an AH patient.

The specific mutations that significantly differed between viral strains derived from the AH and FH patients were first examined. Throughout the HBV genome, there were only three mutations correlated with the severity of the acute type B liver disease. The occurrence of the T1762/A1764 mutation in the BCP was significantly higher in the FH-related strains (5 of 6, 83%) than in the AH-related ones (2 of 9, 22%) ($p < 0.05$). Patients with FH tended to be more frequently infected with the virus possessing the precore-defective A1896 mutation and the M1753 (M = C or A) mutation in the BCP than those with AH (67 vs. 11%, $p = 0.09$ for the A1896 and 67 vs. 11%, $p = 0.09$ for the M1753), though the difference did not reach a statistically significant level.

Next, we tried to evaluate the degree of mutation in HBV strains obtained from the patients with AH and FH. For this purpose, the number of nucleotide substitutions per site (evolutional distance) of each HBV strain was calculated in comparison with the reference HBV strain. To standardize the values of the number of nucleotide substitutions in different subgenotypes of HBV strains, the respective reference HBV strains of subgenotypes A2/Ae, B1/Bj, B2/Ba, C1/Cs and C2/Ce were employed. These reference HBV strains, except for the subgenotype C1/Cs AF223954 strain, had been cloned in the 1980s by means of a non-PCR method and originated from the plasma/serum sample of a single or a plural number of highly viremic chronic HBV carrier(s) [19, 20, 22]. The remaining subgenotype C1/Cs reference strain has recently been identified by PCR from an HBeAg-positive HBV carrier [21]. Thus, all reference HBV strains used for this study had been derived from patients at an early phase of chronic HBV infection, and did not appear to have mutations accompanied by the disease progression. Then, the number of nucleotide substitutions of each HBV strain was calculated for comparison with the corresponding reference HBV strain of the same subgenotype.

The results of the comparison in the number of nucleotide substitutions of the whole or portions of the HBV genome between AH- and FH-related HBV strains are shown in figure 2. The number of nucleotide substitutions in the whole HBV genome was significantly higher in strains from FH patients (median 0.0295 [range 0.0186–0.0347]/site) than in those from AH ones (median 0.0157 [range 0.0072–0.0292]/site) ($p < 0.01$). When the number of nucleotide substitutions in various regions of the HBV genome was studied, the higher number of nucleotide substitutions in the FH-related strains than in the AH-related ones was also observed for the preS/S gene (median 0.0185 [range 0.0150–0.0211]/site vs. median 0.0101 [range 0.0075–0.0203]/site, $p < 0.05$), precore/core gene (median 0.0354 [range 0.0174–0.0742]/site vs. median 0.0110 [range 0.0047–0.0271]/site, $p < 0.01$) polymerase gene (median 0.0266 [range 0.0172–0.0315]/site vs. median 0.0164 [range 0.0067–0.0294]/site, $p < 0.05$) and BCP/core upstream regulatory sequence (CURS) [27] (median 0.0333 [range 0.0188–0.0429]/site vs. median 0.0093 [range 0.0046–0.0285]/site, $p < 0.01$), but not in the X gene.

The codon-by-codon numbers of nucleotide synonymous and non-synonymous substitutions (d_S and d_N) between each of the HBV strains obtained in this study and the reference strain were studied further (table 2). In the preS/S gene, the d_N value but not the d_S value was significantly higher in strains from the FH patients than in

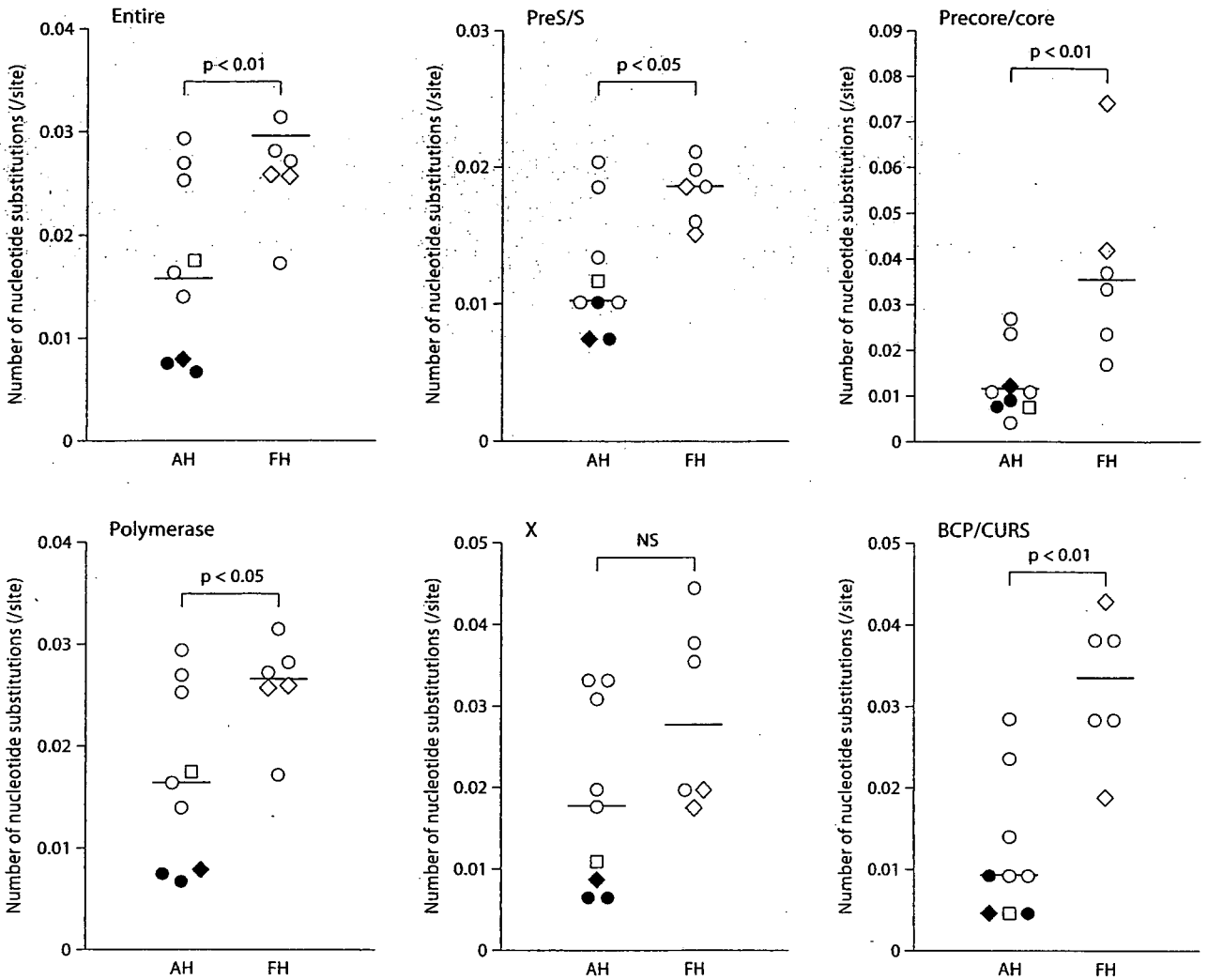

Fig. 2. Number of nucleotide substitutions per site in the entire and various regions of HBV genome in strains from patients with AH and FH. ○ = Subgenotype C2/Ce HBV strains; ●, ◇, ◆, □ = HBV strains of subgenotypes A2/Ae, B1/Bj, B2/Ba and C1/Cs, respectively.

Table 2. Numbers of nucleotide synonymous and non-synonymous substitutions in various genes of AH- and FH-related HBV strains

Genomic regions of HBV	Number of synonymous substitutions (d_S) (/synonymous site)			Number of non-synonymous substitutions (d_N) (/non-synonymous site)		
	AH	FH	p value	AH	FH	p value
PreS/S	0.0271 (0.0101–0.0516)[1]	0.0351 (0.0270–0.0410)	NS[2]	0.0067 (0.0033–0.0146)	0.0121 (0.0082–0.0150)	<0.05
Precore/core	0.0418 (0.0185–0.0683)	0.0771 (0.0515–0.1311)	<0.05	0 (0–0.0032)	0.0184 (0.0064–0.0546)	<0.005
Polymerase	0.0361 (0.0096–0.0646)	0.0611 (0.0353–0.0681)	<0.05	0.0099 (0.0047–0.018)	0.0150 (0.0112–0.0216)	NS
X	0.0344 (0–0.0704)	0.0503 (0.0252–0.0796)	NS	0.0148 (0–0.0209)	0.0187 (0.0089–0.0331)	NS

[1] Values are expressed as median (range). [2] NS = not significant.

those from the AH ones. The FH-related strains showed both higher d_S and d_N values than the AH-related ones in the precore/core gene ($p < 0.05$ for the d_S value and $p < 0.005$ for the d_N value), and the difference of the d_N value was more prominent than that of the d_S value between strains from AH and FH patients. As for the polymerase gene, only the d_S value was significantly higher in viruses infecting FH patients than in those infecting AH ones ($p < 0.05$). Neither the d_S value nor the d_N value in the X gene differed between the strains from the AH and FH patients.

Discussion

In the present study, we carried out sequencing analysis of full-length HBV DNA derived from a considerable number of patients with type B AH and FH. We attempted to validate genome-wide features in the FH-related HBV strains. The mutation hotspots associated with FH were first investigated through screening of the entire HBV genome. It was found that FH-related viral strains tended to have the T1762/A1764 mutation in the BCP, the A1896 mutation in the precore gene and the M1753 mutation in the BCP more frequently than the AH-related ones. This is consistent with previous reports [3, 4, 7–9], though it has not been fully understood why the viruses with these mutations link to the serious disease course in the acute HBV infection. It is also of note that no other particular mutations related to development of FH were observed throughout the HBV genome.

Our 15 HBV strains encompassed five different subgenotypes, A2/Ae, B1/Bj, B2/Ba, C1/Cs and C2/Ce. It has recently been shown in a large-scale study from Japan that patients with FH were infected less frequently with the subgenotype A2/Ae virus and more frequently with the subgenotype B1/Bj virus than those with AH [9]. Indeed, the subgenotype A2/Ae was detected in only two AH-related strains, whereas the subgenotype B1/Bj was seen in only two FH-related strains in this study. Thus, the HBV subgenotype may be one of the determining factors for prognosis of the acute HBV infection.

Next, we evaluated the number of nucleotide substitutions as an index of the degree of the mutation in each of the viral strains obtained in this study in comparison with the reference HBV strain. The values of the number of nucleotide substitutions were standardized by setting up the respective reference HBV strain of each subgenotype to overcome sequence variability among subgenotypes. The number of nucleotide substitutions was shown to be significantly higher in the FH-related strain than in the AH-related ones for the whole genome and various regions (preS/S, precore/core, polymerase and BCP/CURS) of HBV. Our finding indicates that development of type B FH may be closely associated with a highly mutated HBV strain, whose mutations occur in a wide range of the viral genome. Several investigators have examined the nucleotide sequences of full-length HBV strains derived from a limited number of FH patients, and most of these FH-related HBV strains differed considerably in nucleotide and amino acid sequences when they were compared with the previously reported consensus HBV strain [10–15]. However, these previous studies were not comparative ones and did not examine sequence information of the viral genome derived from AH patients. As the present study analyzed the HBV sequences derived from a considerable number of patients of both AH and FH, our findings should offer more reliable information regarding the difference between AH and FH strains. Our observations indicate that a highly mutated HBV strain may be one of the important etiologic causes of type B FH.

The BCP/CURS region [27], which overlaps the enhancer II region [28, 29], is known to regulate the viral transcription via interaction of cellular transcription factors with their specific DNA elements. In this study, the number of nucleotide substitutions in the BCP/CURS region was found to be higher in viruses from the FH than AH patients. This region includes three mutation hotspots (nt positions 1753, 1762 and 1764) associated with FH as described above. In addition, a few investigators have identified the strain-specific mutation/insertion occurring in the BCP other than the hotspot mutations as the accountable genomic change for development of FH [11, 15, 30]. Baumert et al. [30] have demonstrated that the HBV strain derived from an FH patient [11] showed more than tenfold higher viral replication, and that the enhanced viral encapsidation activity of the strain was caused by the T1766/A1768 mutation. More recently, transfection with the HBV strain having the T1766/A1768 mutation has also been reported to induce more apoptosis in primary *Tupaia* hepatocytes than that with the wild-type HBV strain [31]. It has also been shown by Pult et al. [15] that the HBV strain isolated from a heart transplant recipient who developed the transplant-transmitted FH had the 11-bp insertion in the BCP, leading to enhanced viral transcription and replication via generation of the novel hepatocyte nuclear factor 1 binding site. Taken together, the hypermutation in the BCP/CURS region including the hotspot mutations and other types of genomic changes may be involved in the pathogenesis of type B FH.

In the present study, we further studied the numbers of nucleotide synonymous and non-synonymous substitutions (d_S and d_N) in each viral strain in the four open reading frames of HBV. The higher number of nucleotide substitutions in the FH-related strains compared with the AH-related ones was found to be predominantly non-synonymous in the precore/core and preS/S genes. By contrast, in the polymerase and X genes, no significant differences in the number of non-synonymous substitutions were observed between strains from AH and FH patients. The precore/core and preS/S proteins are known to include epitopes against the humoral and cellular immune responses of the host. The high incidence of the amino acid substitutions in these viral structural proteins may cause a hyperimmune response, resulting in enhanced hepatocyte injury and development of FH.

It is debatable whether many viral mutations occurring in the FH-related strains would appear before infection or during development of FH after infection. It is currently conceivable that the high incidence of non-synonymous mutations compared to synonymous ones reflects the positive selection. In the precore/core and preS/S genes, the difference in the d_N value the between AH- and FH-related strains was more prominent than that in the d_S value, suggesting that the strong positive selection in these genes may occur in the FH patients than in the AH ones. With respect to this, the possibility cannot be excluded that mutations occurred in the precore/core and preS/S genes may be rapidly emerged in the acutely infected patients as a consequence of the strong intrahost selection. On the other hand, the d_S value also tended to be higher in the viruses derived from FH patients than in those from AH ones, especially in the polymerase gene. This indicates that at least a portion of the mutations in the FH-related viral strain may occur presumably in the HBV carrier of an infectious source before transmission of HBV, because synonymous mutations generally occur in time irrespective of the selective pressure within the host.

We also showed that a substantial number of mutations can occur even in the viral strains derived from AH patients, compared with the reference strain. Some of the AH-related strains possessed a considerably high rate of mutations in the HBV genome. According to this, a highly mutated HBV strain may be a necessary, but not a sufficient, factor for development of FH. Accumulation of various viral and host factors may be involved in the pathogenesis of type B FH. Further studies are required to clarify this.

In summary, our full-length sequencing study of HBV strains derived from a considerable number of patients with AH and FH revealed a close relationship of the highly mutated HBV strain with the development of FH. In particular, our findings suggest that the hypermutation in the BCP/CURS region and the high incidence of the amino acid-substituting mutation in the precore/core and preS/S genes may be relevant to the pathogenesis of type B FH.

References

1 Lee WM: Acute liver failure. N Engl J Med 1993;329:1862–1872.
2 Carman WF, Jacyna MR, Hadziyannis S, Karayiannis P, McGarvey MJ, Makris A, Thomas HC: Mutation preventing formation of hepatitis B e antigen in patients with chronic hepatitis B infection. Lancet 1989;2:588–2591.
3 Omata M, Ehata T, Yokosuka O, Hosoda K, Ohto M: Mutations in the precore region of hepatitis B virus DNA in patients with fulminant and severe hepatitis. N Engl J Med 1991;324:1699–1704.
4 Liang TJ, Hasegawa K, Rimon N, Wands JR, Ben-Porath E: A hepatitis B virus mutant associated with an epidemic of fulminant hepatitis. N Engl J Med 1991;324:1705–1709.
5 Okamoto H, Tsuda F, Akahane Y, Sugai Y, Yoshiba M, Moriyama K, Tanaka T, Miyakawa Y, Mayumi M: Hepatitis B virus with mutations in the core promoter for an e antigen-negative phenotype in carriers with antibody to e antigen. J Virol 1994;68:8102–8110.
6 Buckwold VE, Xu Z, Chen M, Yen TS, Ou JH: Effects of a naturally occurring mutation in the hepatitis B virus basal core promoter on precore gene expression and viral replication. J Virol 1996;70:5845–5851.
7 Sato S, Suzuki K, Akahane Y, Akamatsu K, Akiyama K, Yunomura K, Tsuda F, Tanaka T, Okamoto H, Miyakawa Y, Mayumi M: Hepatitis B virus strains with mutations in the core promoter in patients with fulminant hepatitis. Ann Intern Med 1995;122:241–248.
8 Imamura T, Yokosuka O, Kurihara T, Kanda T, Fukai K, Imazeki F, Saisho H: Distribution of hepatitis B viral genotypes and mutations in the core promoter and precore regions in acute forms of liver disease in patients from Chiba, Japan. Gut 2003;52:1630–1637.
9 Ozasa A, Tanaka Y, Orito E, Sugiyama M, Kang JH, Hige S, Kuramitsu T, Suzuki K, Tanaka E, Okada S, Tokita H, Asahina Y, Inoue K, Kakumu S, Okanoue T, Murawaki Y, Hino K, Onji M, Yatsuhashi H, Sakugawa H, Miyakawa Y, Ueda R, Mizokami M: Influence of genotypes and precore mutations on fulminant or chronic outcome of acute hepatitis B virus infection. Hepatology 2006;44:326–334.
10 Ogata N, Miller RH, Ishak KG, Purcell RH: The complete nucleotide sequence of a precore mutant of hepatitis B virus implicated in fulminant hepatitis and its biological characterization in chimpanzees. Virology 1993;194:263–276.
11 Hasegawa K, Huang J, Rogers SA, Blum HE, Liang TJ: Enhanced replication of a hepatitis B virus mutant associated with an epidemic of fulminant hepatitis. J Virol 1994;68:1651–1659.

12 Asahina Y, Enomoto N, Ogura Y, Sakuma I, Kurosaki M, Izumi N, Marumo F, Sato C: Complete nucleotide sequences of hepatitis B virus genomes associated with epidemic fulminant hepatitis. J Med Virol 1996;48: 171–178.
13 Alexopoulou A, Karayiannis P, Hadziyannis SJ, Hou J, Pickering J, Luo K, Thomas HC: Whole genome analysis of hepatitis B virus from four cases of fulminant hepatitis: genetic variability and its potential role in disease pathogenicity. J Viral Hepat 1996;3: 173–181.
14 Sterneck M, Gunther S, Santantonio T, Fischer L, Broelsch CE, Greten H, Will H: Hepatitis B virus genomes of patients with fulminant hepatitis do not share a specific mutation. Hepatology 1996;24:300–306.
15 Pult I, Chouard T, Wieland S, Klemenz R, Yaniv M, Blum HE: A hepatitis B virus mutant with a new hepatocyte nuclear factor 1 binding site emerging in transplant-transmitted fulminant hepatitis B. Hepatology 1997;25:1507–1515.
16 Trey C, Davidson C: The management of fulminant hepatic failure; in Popper H, Schaffner F (eds): Progress in Liver Disease. New York, Grune & Stratton, 1970, vol 3, pp 282–298.
17 Dai CY, Yu ML, Chen SC, Lin ZY, Hsieh MY, Wang LY, Tsai JF, Chuang WL, Chang WY: Clinical evaluation of the COBAS Amplicor HBV monitor test for measuring serum HBV DNA and comparison with the Quantiplex branched DNA signal amplification assay in Taiwan. J Clin Pathol 2004;57:141–145.
18 Gunther S, Li BC, Miska S, Kruger DH, Meisel H, Will H: A novel method for efficient amplification of whole hepatitis B virus genomes permits rapid functional analysis and reveals deletion mutants in immunosuppressed patients. J Virol 1995;69:5437–5444.
19 Valenzuela P, Quiroga M, Zalvidar J, Gray P, Rutter WJ: The nucleotide sequence of the hepatitis B viral genome and the identification of the major viral genes; in Fields BN, Jaenisch R, Fox CF (eds): Animal Virus Genetics. New York, Academic Press, 1980, pp 57–70.
20 Okamoto H, Tsuda F, Sakugawa H, Sastrosoewignjo RI, Imai M, Miyakawa Y, Mayumi M: Typing hepatitis B virus by homology in nucleotide sequence: comparison of surface antigen subtypes. J Gen Virol 1988;69:2575–2583.
21 Alestig E, Hannoun C, Horal P, Lindh M: Phylogenetic origin of hepatitis B virus strains with precore C-1858 variant. J Clin Microbiol 2001;39:3200–3203.
22 Fujiyama A, Miyanohara A, Nozaki C, Yoneyama T, Ohtomo N, Matsubara K: Cloning and structural analyses of hepatitis B virus DNAs, subtype adr. Nucleic Acids Res 1983; 11:4601–4610.
23 Kimura M: A simple method for estimating evolutionary rates of base substitutions through comparative studies of nucleotide sequences. J Mol Evol 1980;16:111–120.
24 Saitou N, Nei M: The Neighbor-Joining Method. A new method for estimating and testing minimum-evolution trees. Mol Biol Evol 1987;4:406–425.
25 Nei M, Gojobori T: Simple method for estimating the numbers of synonymous and nonsynonymous nucleotide substitutions. Mol Biol Evol 1986;3:418–426.
26 Kumar S, Tamura K, Nei M: MEGA3: integrated software for Molecular Evolutionary Genetics Analysis and sequence alignment. Brief Bioinform 2004;5:150–163.
27 Yuh CH, Chang YL, Ting LP: Transcriptional regulation of precore and pregenomic RNAs of hepatitis B virus. J Virol 1992;66: 4073–4084.
28 Su H, Yee JK: Regulation of hepatitis B virus gene expression by its two enhancers. Proc Natl Acad Sci USA 1992;89:2708–2712.
29 Yuh CH, Ting LP: The genome of hepatitis B virus contains a second enhancer: cooperation of two elements within this enhancer is required for its function. J Virol 1990;64: 4281–4287.
30 Baumert TF, Rogers SA, Hasegawa K, Liang TJ: Two core promoter mutations identified in a hepatitis B virus strain associated with fulminant hepatitis result in enhanced viral replication. J Clin Invest 1996;98:2268–2276.
31 Baumert TF, Yang C, Schurmann P, Kock J, Ziegler C, Grullich C, Nassal M, Liang TJ, Blum HE, von Weizsacker F: Hepatitis B virus mutations associated with fulminant hepatitis induce apoptosis in primary *Tupaia* hepatocytes. Hepatology 2005;41:247–256.

Available online at www.sciencedirect.com
ScienceDirect
Virology 367 (2007) 126–134
VIROLOGY
www.elsevier.com/locate/yviro

Cryo-electron microscopy and three-dimensional reconstructions of hepatitis C virus particles

Xuekui Yu [a,2], Ming Qiao [b,1], Ivo Atanasov [a], Zongyi Hu [b], Takanobu Kato [b], T. Jake Liang [b,*,2], Z. Hong Zhou [a,2]

[a] *Department of Pathology and Laboratory Medicine, The University of Texas Medical School at Houston, Houston, TX 77030, USA*
[b] *Liver Diseases Branch, National Institute of Diabetes and Digestive and Kidney Diseases, National Institutes of Health, Bethesda, MD 20892, USA*

Received 23 March 2007; returned to author for revision 4 May 2007; accepted 9 May 2007
Available online 5 July 2007

Abstract

The structural details of hepatitis C virus (HCV) have been elusive because of the lack of a robust tissue culture system for producing an adequate amount of virions from infectious sources for in-depth three-dimensional (3D) structural analysis. Using both negative-stain and cryo-electron microscopy (cryoEM), we show that HCV virions isolated from cell culture have a rather uniform size of 500 Å in diameter and that recombinantly expressed HCV-like particles (HCV-LPs) have similar morphologic, biophysical and antigenic features in spite of the varying sizes of the particles. 3D reconstructions were obtained from HCV-LPs with the same size as the HCV virions in the presence and absence of monoclonal antibodies bound to the E1 glycoprotein. The 3D reconstruction of HCV-LP reveals a multilayered architecture, with smooth outer-layer densities arranged in a 'fishbone' configuration. Reconstruction of the particles in complex with anti-E1 antibodies shows that sites of the E1 epitope are exposed and surround the 5-, 3- and 2-fold axes. The binding pattern of the anti-E1 antibody and the fitting of the structure of the dengue virus E glycoprotein into our 3D reconstructions further suggest that the HCV-LP E1 and E2 proteins form a tetramer (or dimer of heterodimers) that corresponds morphologically and functionally to the flavivirus E homodimer. This first 3D structural analysis of HCV particles offers important insights into the elusive mechanisms of HCV assembly and maturation.

Keywords: Assembly; Envelope protein; Nucleocapsid; Neutralizing antibodies; Viral infection

Introduction

HCV infects more than 170 million people worldwide and causes persistent infection in more than 70% of infected people (Liang et al., 2000). It is the world's leading cause of chronic liver disease and liver cancer. HCV is a member of the Flaviviridae family but has been classified into its own genus, *Hepacivirus*, because of major differences in genomic organization and amino acid sequences from viruses in the *Flavivirus* genus, such as dengue virus and West Nile virus (collectively called flaviviruses). HCV has a positive-strand RNA genome of about 9.5 kb, which encodes a large polyprotein that is processed to structural and non-structural proteins by the viral and cellular proteases. The structural proteins of HCV reside at the N-terminus of the polyprotein, but unlike flaviviruses, HCV encodes two distinct envelope glycoproteins, E1 and E2, and notably lacks a structural or functional homolog of the prM/M protein found in flaviviruses.

It has been difficult to grow HCV in tissue culture, and only recently were infectious HCV virions grown successfully in cell culture (Heller et al., 2005; Lindenbach et al., 2005; Wakita et al., 2005; Zhong et al., 2005). However, none of the existing systems produce viral particles of adequate quantity and quality for three-dimensional (3D) structural analysis. Indeed, no direct structural information about HCV has been available until now and our understanding of HCV structure has only been gleaned through extrapolation of data from analyses of structural proteins

* Corresponding author. Fax: +1 301 402 0491.
E-mail address: jliang@nih.gov (T.J. Liang).
[1] Present address: Infectious Diseases Laboratories, Institute of Medical and Veterinary Science, Adelaide, South Australia 5000, Australia.
[2] These authors contributed equally to this work.

0042-6822/$ - see front matter © 2007 Published by Elsevier Inc.
doi:10.1016/j.virol.2007.05.038

expressed by alternative systems (Kunkel et al., 2001; Kunkel and Watowich, 2002). As a result, very little is known about the structural organization of HCV. This is in stark contrast to other members of the Flaviviridae family, such as the dengue virus (Kuhn et al., 2002; Modis et al., 2003, 2004; Pokidysheva et al., 2006), tick-borne encephalitis virus (Ferlenghi et al., 2001; Rey et al., 1995) and West Nile virus (Kanai et al., 2006; Mukhopadhyay et al., 2003), whose structures have been studied extensively by both cryo-electron microscopy (cryoEM) and X-ray crystallography.

In this study, we first show that the HCV virions isolated from cell culture have a rather uniform size distribution with a predominant diameter of ~500 Å by cryoEM and negative-stain electron microscopy. However, these HCV virions were not appropriate for 3D reconstruction analysis due to their limited quantity. Using a baculovirus system to express the structural proteins of HCV, we produced large amounts of HCV-like particles (HCV-LPs) similar to HCV virions by biochemical, cryoEM and immunogold electron microscopy analyses. 3D reconstructions of the HCV-LP and their complexes bound with anti-E1 antibodies show a structural organization similar to those of the dengue and West Nile viruses. Fitting of the atomic model of dengue virus E protein into our cryoEM maps further reveals some key structural differences between HCV-LP and the flaviviruses that are consistent with the unique aspects of the chemical composition and viral assembly known for HCV.

Results and discussion

Wild-type HCV virion has a predominant size of 500 Å in diameter

The biochemistry of HCV has been studied extensively since it was first discovered in 1989, but its morphology and size remained controversial. We have successfully isolated some HCV virions from cell culture and obtained electron microscopy images of purified HCV virions, both by negative-stain transmission electron microscopy (TEM) (Fig. 1A) and cryoEM (Fig. 1B). Our images show that the sizes of the HCV virions purified from cell culture are quite uniform, having a diameter of about 500 Å as measured from the cryoEM images (Fig. 1B). In the cryoEM preparation in particular, the HCV virions were preserved in a frozen hydrated state. Since there is no size and structure distortion due to staining and drying artefacts possible in negative-stain TEM, our data directly establishes that infectious HCV virion particles have a predominant size of ~500 Å. Despite this encouraging result, the quantity and quality of the HCV virions isolated from cell culture remain limited and insufficient for in-depth 3D reconstruction. Nonetheless, our EM images clearly demonstrated that HCV virions isolated from cultured cells have a rather uniform diameter of around 500 Å and with a smooth or spikeless outer surface (Fig. 1B). Thus, HCV shares a size and morphology with other structurally well characterized members of the Flaviviridae, such as the dengue virus (Kuhn et al., 2002) and West Nile virus (Mukhopadhyay et al., 2003).

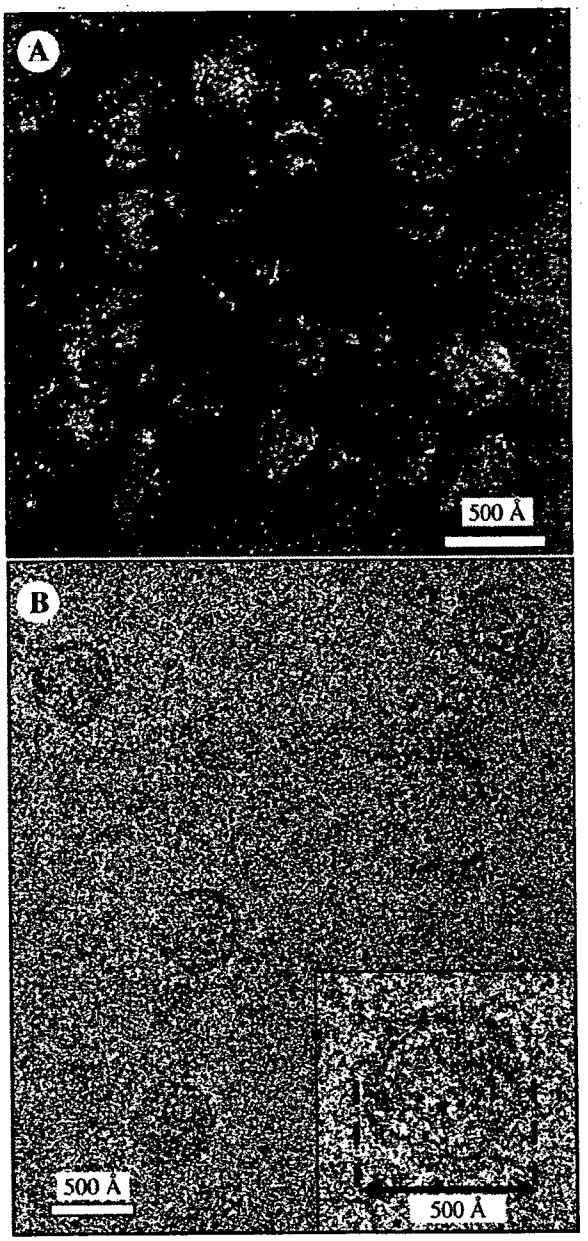

Fig. 1. Electron microscopy of HCV virions purified from cell culture. JFH-1 HCV virions were produced in cell culture and purified by iodixanol density gradient centrifugation as described in Materials and methods. (A) Negative-stain TEM micrograph shows that the HCV virions have a rather uniform size distribution. (B) CryoEM images of HCV virions embedded in vitreous ice. Because there are no staining and drying artifacts, these cryoEM images of the HCV virions establish their size of ~500 Å in diameter and show a smooth surface morphology with a multilayer outer structural organization (see inset) similar to that of the mature virions of the dengue and West Nile viruses (Kuhn et al., 2002; Mukhopadhyay et al., 2003).

Cryo-electron microscopy and biochemical analyses of HCV-like particles

To overcome the difficulties in obtaining sufficient amount of materials needed for in-depth biochemical and cryoEM structural analyses, we took advantage of the previous success

in generating large quantities of HCV-LPs in insect cells (Qiao et al., 2004). HCV-LPs were isolated by iodixanol density gradient centrifugation from insect cells infected with recombinant baculovirus expressing HCV structural proteins. CryoEM examination of the fraction containing the highest concentration of HCV structural proteins revealed spherical particles with smooth surfaces (Fig. 2A), consistent with the purified wild-type HCV virions seen in Fig. 1 and the native HCV virions isolated from HCV infected patients (Prince et al., 1996; Trestard et al., 1998), although the recombinant HCV-LPs are more heterogeneous as judged by particle size distribution (Figs. 2A, B). This heterogeneity might be due to incorporation of variable units of HCV E1–E2 dimers during assembly of HCV-LP. Western blot analysis confirmed that the HCV-LPs are composed of all three HCV structural proteins (E1, E2 and C) (Fig. 2C). The different molecular weights of the E1 protein likely result from different extents of glycosylation.

We next examined the HCV structure by labeling the HCV-LP with monoclonal antibodies against the HCV E1 protein. CryoEM images of the antibody-labeled HCV-LPs showed very prominent spikes decorating particles of different sizes (arrows in Fig. 2D). Collectively, these density spikes form a ring surrounding the underlying smooth particles (Fig. 2D), indicating binding of the antibody to HCV-LP. Double-antibody labeling experiments using monoclonal antibodies against E1 and secondary gold-conjugated anti-IgG antibodies confirmed that the anti-E1 monoclonal antibody binds to HCV-LPs (Fig. 2E). These labeling experiments confirmed that the outer layer of the HCV-LP contains E1 protein with its epitope exposed on the outer surface. As expected, prominent particle aggregation was also observed in the antibody-labeled HCV-LP experiments as a consequence of antibody cross-linking (Figs. 2D, E).

Previous biochemical studies have suggested that the HCV E1 and E2 proteins form heterodimers during the assembly process (Dubuisson, 2000). Other studies using monoclonal antibodies against E1 and E2 have suggested that the E1–E2 complexes form the outer surfaces of the native HCV particles, HCV-LPs and infectious pseudotyped HCV particles (Bartosch et al., 2003; Meyer et al., 2004; Petit et al., 2005; Prince et al., 1996; Triyatni et al., 2002a, 2002b). Our results provide the first

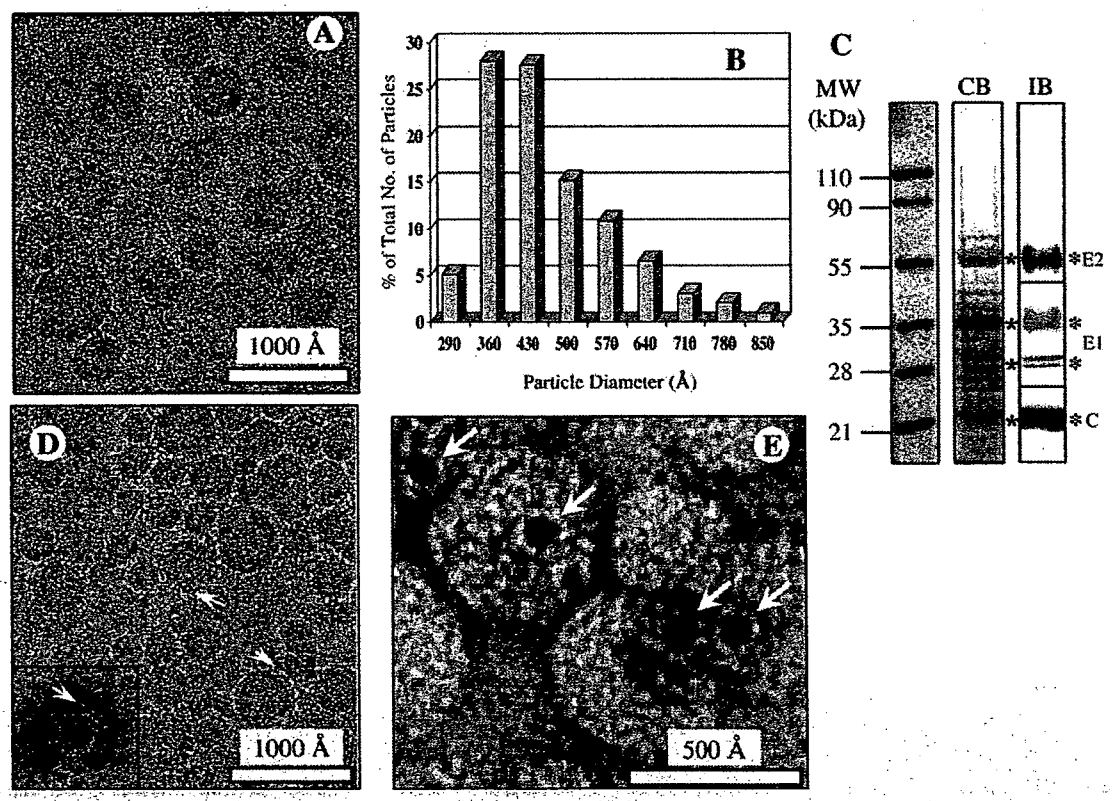

Fig. 2. CryoEM and immunogold TEM of HCV-LPs. (A) Representative area of a typical cryoEM micrograph of HCV-LPs. The frozen-hydrated HCV-LPs exhibited structural flexibility and size heterogeneity but many of the particles have a size similar to that of the HCV virions isolated in cell culture as seen in Fig. 1. The defocus value was determined to be 1.7 μm underfocus for this image. (B) Distribution profile of HCV-LP diameters in the cryoEM micrographs based on a total number of 1750 particles. (C) Chemical composition of HCV-LP. SDS–PAGE (Coomassie blue staining) and Western blotting (IB) of HCV-LPs detected the presence of the HCV structural proteins C, E1 and E2 (marked by asterisks). MW, molecular weight standard. (D) Representative cryoEM image of HCV-LPs in complex with monoclonal anti-E1 antibodies. The defocus value was determined to be 1.9 μm underfocus for this image. Characteristic spikes attributed to bound antibody molecules (indicated by arrows) can be seen forming a ring of densities about HCV-LPs. The inset shows a negative-stain TEM image of an antibody-decorated HCV-LP from the same antibody-labeled HCV-LP preparation. The densities attributed to the bound antibodies (indicated by the arrow) in the negative-stain image are more clearly visible than in the cryoEM image. (E) Immunogold TEM of anti-E1 antibody decorated HCV-LPs confirming anti-E1 labeling of HCV-LPs. The negative-stain TEM image shows that gold particles bind (black dots pointed by white arrows) anti-E1-labeled HCV-LPs when they were probed with gold-conjugated secondary antibodies.

direct evidence corroborating that E1, likely in complex with E2, indeed form the outer layer of HCV-LP.

3D reconstructions of HCV-LP and antibody-labeled HCV-LP

As demonstrated above, HCV virions isolated from tissue culture have a rather uniform diameter of 500 Å (Fig. 1). Negative-stain TEM of native HCV particles from patient serum has also shown the existence of 500-Å-diameter particles (Prince et al., 1996). Moreover, native dengue and West Nile virus particles have a diameter of 500 Å (Kuhn et al., 2002; Mukhopadhyay et al., 2003). Therefore, despite of variations in particle sizes in the HCV-LP preparation (Figs. 2A, B), we decided to focus on the predominant 500-Å particles for in-depth data processing and 3D reconstruction to facilitate the structural comparison with those of the dengue and West Nile virus. A 3D model was reconstructed to a resolution of 30 Å (Fig. 3B). The convergence of our extensive phase-residue-based refinement and a stable final 3D reconstruction (see details in Materials and methods) is indicative of the existence of icosahedral symmetry in selected HCV-LP. The shaded surface representation of this structure shows a smooth outer shell with surface indentations (Fig. 3B) and characteristic internal membrane structures (Fig. 3C) reminiscent of the arrangement of E proteins in dengue virus and other flaviviruses (Ferlenghi et al., 2001; Kuhn et al., 2002; Mukhopadhyay et al., 2003). Careful interactive examination of the 3D density distribution of the 3D reconstruction revealed a similar structural organization of 90 structural components organized in a 'fishbone' configuration, which has been well established for other members of the Flaviviridae (Kuhn et al., 2002; Mukhopadhyay et al., 2003). The similarity between our reconstruction and other flavivirus structures support the hypothesis that HCV-LP has icosahedral symmetry. Density slices extracted from the 3D reconstruction reveal that the HCV-LP has a multilayer structural organization (Fig. 3C). The outer layer, which we interpret to be the E1–E2 protein layer, is about 30 Å thick and has the highest density as expected for densely packed glycoproteins.

Our interpretation of E1–E2 outer layer is confirmed by 3D structural analysis of the anti-E1-labeled HCV-LPs. Consistent with the TEM observations (Figs. 2D, E), the 3D reconstruction of antibody-labeled HCV-LPs (Fig. 3D) showed extra densities attached to the outer E1–E2 layer (pink in Fig. 3E). A density slice extracted from the antibody-labeled HCV-LP reconstruction (Fig. 3F) revealed a multilayer structural organization similar to that of the unlabeled HCV-LP reconstruction (Fig. 3C). Notably, surrounding the putative E1–E2 shell in this reconstruction is an extra layer of lower density, which most likely is due to the E1-bound antibody molecules. Although the values of the antibody-attributed densities are significantly above background level, they are lower than the E1/E2 densities (Fig. 3F), indicating a low occupancy of the available binding sites and/or flexibility of the bound antibody molecules. Low antibody occupancy and antibody flexibility can be due to a number of reasons, including steric hindrance of the binding sites, low affinity of the antibody and the flexible hinge regions of individual IgG molecules. Each antibody density is attached to the E1–E2 shell at three regions: around the 5-fold axes, near the icosahedral 3-fold axes and flanking the 2-fold axes (Fig. 3F). These sites roughly coincide with the small protrusions seen at the 5-, 3- and 2-fold axes of the dengue virus reconstruction at a similar resolution (Kuhn et al., 2002), although such protrusions were not visible in the HCV-LP reconstruction. This observation suggests that the HCV E1–E2 heterodimer may be organized in a way similar to that of the E monomer of the flaviviruses. In HCV-LP, each E1 molecule closely interacts with an E2 protein to form an E1–E2 heterodimer. Two E1–E2 heterodimers further assemble into a tandem tetramer, which in turn serves as the basic building block of the smooth outer surface of the HCV particle.

Below the E1–E2 layer are two lower-density layers separated by a 40- to 45-Å space (Figs. 3C, F), consistent with the expected thickness of a lipid bilayer. Although the E1–E2 protein densities contact and, in certain regions, extend through the underlying envelope bilayer, there is a clear delineation between the E1–E2 density layer and the lipid bilayer. The distance between the E1–E2 layer and the outer leaflet of the bilayer membrane is around 30 Å, similar to that of flaviviruses (Ferlenghi et al., 2001; Kuhn et al., 2002). In addition, the HCV-LP membrane bilayer appeared to be affected by the overlying icosahedral E1–E2 protein layer, adopting a slightly polygonal shape instead of the typical spherical shape expected for a free lipid vesicle. Similar to observations made in the structural studies of the dengue virus (Zhang et al., 2003a, 2003b), the internal densities corresponding to the capsid core appeared to be asymmetrically organized and were not clearly resolved in our HCV-LP reconstruction. Unlike flaviviruses (Ferlenghi et al., 2001; Kuhn et al., 2002), the HCV-LP reconstruction lacks a discernable intermediate M protein layer between the E1–E2 layer and the lipid bilayer.

HCV model and comparison with flaviviruses

A structural model of the HCV E2 protein has been proposed using sequence alignment and fold recognition methods based on the crystal structure of the tick-borne encephalitis virus (TBEV) soluble E protein (Yagnik et al., 2000). In this model, the ectodomain (aa 384–661) of HCV E2 protein is analogous to domains I and II of the TBEV E protein and the HCV E1 protein presumably represents domain III of the TBEV E protein. Our reconstruction of HCV-LP and the identification of E1 antibody binding sites on the outer surface suggest that the outer shell of the mature HCV virion is composed of dimers of E1–E2 heterodimers in a head-to-tail tandem configuration (Fig. 3). That is, each HCV E1–E2 heterodimer is analogous to a monomer of flavivirus E protein, and each dimer of E1–E2 heterodimers in HCV-LP structurally resembles a flavivirus E-protein homodimer.

Based on the HCV E2 protein model (Yagnik et al., 2000), genomic comparison of HCV and flaviviruses (Figs. 4A, B) and our 3D reconstructions of HCV-LP (Figs. 3B, C) and E1

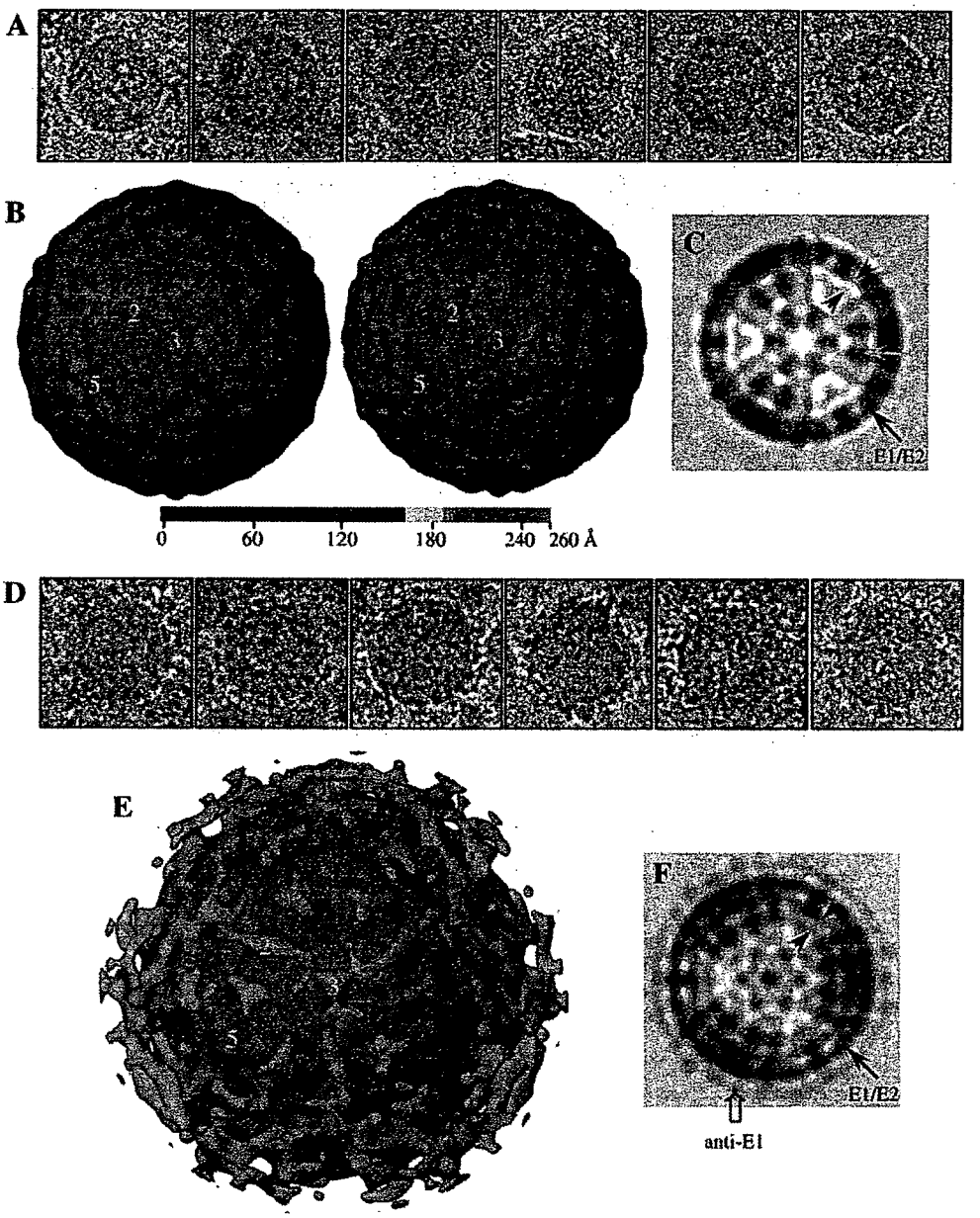

Fig. 3. 3D reconstructions of unlabeled and antibody-labeled 500-Å HCV-LPs. (A) Boxed-out cryoEM images of unlabeled HCV-LPs from the 500-Å size group. (B) Shaded surface representation of the 3D reconstruction of HCV-LP at 30-Å resolution, viewed along an icosahedral 3-fold axis. Densities in panels B and E are color coded according to radius (color bar). Left, map displayed at a contour level of one standard deviation above the mean density. Right, the same map displayed at a slightly higher density contour level (1.1 times the standard deviation above the mean) to reveal the features with more robust density. (C) A 7-Å-thick density slice extracted from the HCV-LP reconstruction shows multilayer structural organization. The two red arrowheads indicate the lipid bilayer; the blue arrow indicates the capsid. Unlike the dengue virus, the HCV-LP lacks an intermediate density layer corresponding to the M-protein layer. The outer layer (black arrow) is attributed to the E1 and E2 proteins. (D) Boxed-out cryoEM images of antibody-labeled HCV-LPs from the same size group. (E) Shaded surface representation of the 3D reconstruction of antibody-labeled HCV-LP, viewed along an icosahedral 3-fold axis. The putative antibody densities are shown in pink. (F) A density slice extracted from the 3D reconstruction of antibody-labeled HCV-LP. The lipid bilayer and E1/E2 layer are indicated as in panel C. The extra layer of lower density surrounding the particle is attributed to the antibodies.

antibody-bound HCV-LP (Figs. 3E, F), we propose a model for the HCV structural organization (Fig. 4C) in which the E1–E2 tetramer (Fig. 4B) serves as the basic building block of the outer shell. Ninety copies of this building block are arranged in a manner similar to that of the flavivirus E-protein dimers to form an outer shell of 500 Å in diameter (Fig. 4C). The E2 protein of HCV takes the place of domains I and II of the dengue E protein, while the dengue virus E protein domain III is replaced by the E1 protein in HCV. The locations of the E1 protein in the HCV structure model are consistent with the binding sites of the anti-E1 antibodies in our structural studies.